TECHNISCHE UNIVERSITÄT DRESDEN

Fakultät Maschinenwesen Institut für Luft- und Raumfahrttechnik

DLR Design Challenge 2023

AirLive

„**Air** **L**ocated **i**nternet **v**ehicle for **e**mergency”

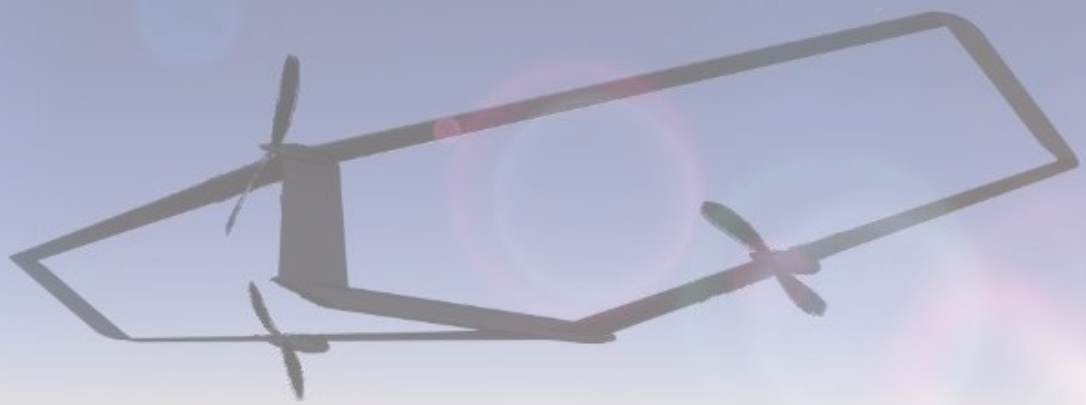

Team

K. Kühmstedt – F. Herrmann – M. Pirags – T. Daenen – T. Garsoffke

Academic Support: Dipl.-Ing. Florian Dexl
Chair of Aircraft Engineering
Technische Universität Dresden

Submission date: 10.07.2023

Declaration of Authorship

We hereby declare that the thesis submitted is our own unaided work.
All direct or indirect sources used are acknowledged as references.

We are aware that the thesis in digital form can be examined for the use of unauthorized aid and in order to determine whether the thesis as a whole or parts incorporated in it may be deemed as plagiarism.

This paper was not previously presented to another board and has not been published.
Dresden, July 10th, 2023

Karl Kühmstedt

Tobias Garsoffke

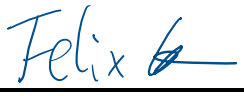

Felix Herrmann

Thijs Daenen

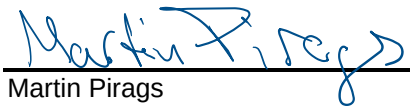

Martin Pirags

Team Members

Karl Kühmstedt
Diploma Student
Aerospace Engineering
6. Semester
karl.kuehmstedt@t-online.de

Tobias Garsoffke
Diploma Student
Aerospace Engineering
6. Semester
tobias.garsoffke@mailbox.tu-dresden.de

Felix Herrmann
Diploma Student
Aerospace Engineering
6. Semester
felix_herrmann1@web.de

Thijs Daenen
Bachelor Student
Aerospace Engineering
6. Semester
thijs.daenen@gmail.com

Martin Pirags
Bachelor Student
Aerospace Engineering
6. Semester
martin.pirags@gmail.com

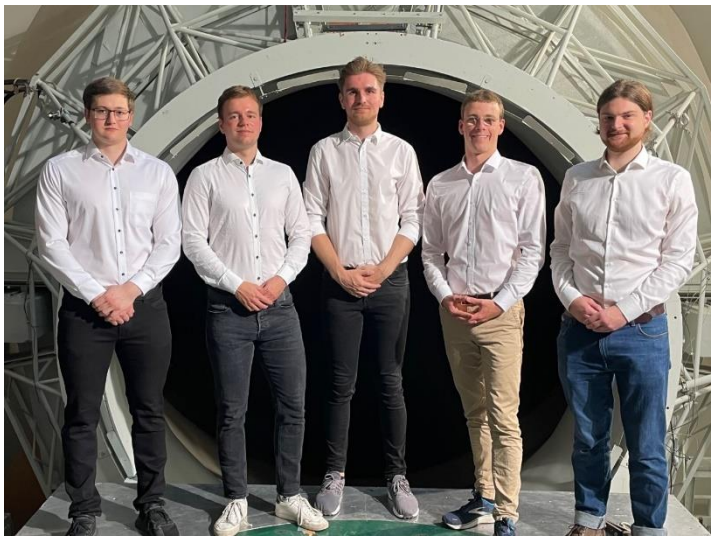

Team AirLive

TECHNISCHE UNIVERSITÄT DRESDEN

Fakultät Maschinenwesen Institut für Luft- und Raumfahrttechnik
Professur für Luftfahrzeugtechnik

Technische Universität Dresden, 01062 Dresden

Deutsches Zentrum für Luft- und Raumfahrt e. V.
(DLR)
Institut für Systemarchitekturen in der Luftfahrt |
Automatisierung, Energie und Sicherheit
c/o ZAL TechCenter
Hein-Saß-Weg 22
21129 Hamburg

Prof. Dr.
Johannes Markmiller
Professur für Luftfahrzeugtechnik
Bearbeitung: Florian Dexl
Wissenschaftlicher Mitarbeiter
Telefon: 0351 463-38096
Telefax: 0351 463-37263
E-Mail: florian.dexl@tu-dresden.de
AZ: 23-08
Datum: 06.07.2023

NASA/DLR Design Challenge: Approval and support of report submission

To whom it may concern,

As the academic supervisors, we hereby declare to approve the report written by the student team consisting of:

- Thijs Daenen,
- Tobias Garsoffke,
- Felix Herrmann,
- Karl Kühmstedt,
- Martin Pirags

and support the submission to the NASA/DLR Design Challenge 2023. We further declare that the report is the result of the above-listed students' own work.

Best regards

Johannes Friedrich Carl Markmiller
Digital unterschrieben von Johannes Friedrich Carl Markmiller
Datum: 2023.07.06 14:03:23 +02'00'

Prof. Dr. Johannes Markmiller

TECHNISCHE UNIVERSITÄT DRESDEN
Institut für Luft- und Raumfahrttechnik
Professur für Luftfahrzeugtechnik
Prof. Dr. Johannes Markmiller
01062 Dresden

Dipl.-Ing. Florian Dexl

Abstract

Due to climate change, the number of storms, hurricanes, blizzards, floods have increase dramatically over the last few years. A consequence might be a failure of the internet infrastructure as critical piece of our everyday life, followed by slow emergency response or even complete failure of ground-based infrastructure. As a solution building and maintaining an emergency satellite network will be prohibitively expensive and depended on private companies.
To provide potential alternatives for emergency communication services, the student team of the Technische Universität Dresden has designed a hydrogen powered air located internet vehicle for emergencies – *AirLive*. This report covers the viability of *AirLive* for an entry into service by 2040, while observing the guidelines of the DLR Design Challenge 2023.
AirLive uses cutting edge technologies and innovative design to enable flexible, quick and efficient operation. Utilizing a box-wing configuration, this concept features high aerodynamic efficiency while flying at high altitudes. Additionally, *AirLive* makes use of an environmentally friendly propulsion system, powering three electrically driven highly efficient propellers. To serve as versatile as possible, a modular design was chosen.

Zusammenfassung

Aufgrund des Klimawandels hat die Anzahl der Stürme, Hurrikans, Schneestürme und Überschwemmungen in den letzten Jahren dramatisch zugenommen. Die Folge könnte ein Ausfall der Internetinfrastruktur als wichtiger Bestandteil unseres alltäglichen Lebens sein, gefolgt von einer langsamen Reaktion auf Notfälle oder sogar einem vollständigen Ausfall der bodengestützten Infrastruktur. Als Lösung wären der Aufbau und die Aufrechterhaltung eines Notfall-Satellitennetzwerks unerschwinglich teuer und von privaten Unternehmen abhängig.
Um potenzielle Alternativen für Notfallkommunikationsdienste anzubieten, hat das Studententeam der Technischen Universität Dresden ein air located internet vehicle for emergencies – *AirLive* entwickelt. Dieser Bericht befasst sich mit der Umsetzbarkeit von *AirLive* für eine Indienststellung bis 2040 unter Beachtung der Richtlinien der DLR Design Challenge 2023.
AirLive nutzt modernste Technologien und innovatives Design, um einen flexiblen, schnellen und effizienten Betrieb zu ermöglichen. Das Konzept nutzt ein Box-Wing-Konfiguration und zeichnet sich durch seine hohe aerodynamische Effizienz beim Fliegen in großen Höhen aus. Darüber hinaus nutzt *AirLive* ein umweltfreundliches Antriebssystem, das drei elektrisch angetriebene, hocheffiziente Propeller antreibt. Um möglichst vielseitig einsetzbar zu sein, wurde ein modularer Aufbau gewählt.

Content

Abbreviations

Abbreviation	Meaning
ADF	aircraft de-icing fluid
AoA	angle of attack
AR	aspect ratio
AC	aircraft
BBIRM	Broadband internet relay modules
CG	center of gravity
CRFP	carbon fibre reinforced plastic
CS	certification specification
DC	direct current
EAS	equivalent airspeed
EASA	European Union Aviation Safety Agentcy
EIS	entry into service
FEU	forty-foot equal unit
FL	flight level
GPS	global positioning system
HH	Hamburg
LED	light emitting diod
LT-PEMFC	low-temperature proton exchange membrane fuel cell
MAC	mean aerodynamic chord
N	neutral point
NFRC	natural fibre reinforced composites
req	required
RPM	revolutions per minute
RPS	revolution per second
SH	Schleswig-Holstein
TAS	true airspeed
TEU	twenty-foot equal unit
TRL	technology readiness level
USA	United States of America
UV	ultraviolet

Nomenclature

Symbol	Meaning	Unit
g	gravitation acceleration	$\frac{\mathrm{m}}{\mathrm{s}^2}$
v	speed	$\frac{\mathrm{m}}{\mathrm{s}}$
m_{TO}	take-off weight	kg
$m_{TO,max}$	maximum take-off weight	kg
S	wing area	m^2
S_1	wing 1 area	m^2
S_2	wing 2 area	m^2
C_L	lift coefficient	$-$
C_{L0}	zero-lift coefficient	$-$
$C_{L\alpha}$	lift curve slope	$-$
α	angle of attack	$°, \mathrm{rad}$
C_D	drag coefficient	$-$
C_{D0}	zero-drag coefficient	$-$
C_{Di}	induced drag coefficient	$-$

SM	Safety Margin	–
h_N	relative neutral point	–
h_{CG}	relative center of gravity in x	–
x_N	neutral point position in x	m
x_{CG}	center of gravity in x	m
$x_{25.1}$	aerodynamic center of wing 1 in x	m
$x_{25.2}$	aerodynamic center of wing 2 in x	m
$y_{25,1}$	aerodynamic center of wing 1 in y	m
$y_{25,2}$	aerodynamic center of wing 2 in y	m
$z_{25,1}$	aerodynamic center of wing 1 in z	m
$z_{25,2}$	aerodynamic center of wing 2 in z	m
C_M	moment coefficient	–
C_{M0}	zero-moment coefficient	–
$C_{M\alpha}$	moment slope coefficient	–
C_{MCG}	moment coefficient about CG	–
M_N	moment about N	Nm
M_{CG}	moment about CG	Nm
M_1	moment of wing 1	Nm
M_2	moment of wing 2	Nm
c, c_{ref}	reference chord length	m
c_{r1}	wing root chord of wing 1	m
c_{r2}	wing root chord of wing 2	m
c_{t1}	wing-tip chord of wing 1	m
c_{t2}	wing-tip chord of wing 2	m
c_{m1}	mean aerodynamic chord of wing 1	m
c_{m2}	mean aerodynamic chord of wing 2	m
ε	downwash angle	°, rad
ψ	dihedral angle	°, rad
θ	incidence angle	°, rad
ϵ	twist angle	°, rad
L	lift	N
L_1	lift of wing 1	N
L_2	lift of wing 2	N
E	glid number	–
E_{max}	maximum glid number	–
k	induced drag factor	–
e	Oswald efficiency factor	–
q	dynamic pressure	$\frac{\text{kg}}{\text{m} \cdot \text{s}}$
ρ_0	air density at sea-level	$\frac{\text{kg}}{\text{m}^3}$
ρ	air density at cruise altitude	$\frac{\text{kg}}{\text{m}^3}$
n	load factor	–
AR	aspect ratio	–
AR_1	aspect ratio of wing 1	–
AR_2	aspect ratio of wing 2	–
b	wingspan	m
ξ	relative length coordinate	–
$\varphi_{25,1}$	quarter chord wing sweep of wing 1	°, rad
$\varphi_{25,2}$	quarter chord wing sweep of wing 2	°, rad
Ma, M	Mach number	–

Ma_{max}	maximum Mach number	$-$
a	speed of sound	$\frac{\mathrm{m}}{\mathrm{s}}$
π	circle number	$-$
h	cruise altitude or altitude	m
λ_1	taper ratio of wing 1	$-$
λ_2	taper ratio of wing 2	$-$
γ	climb gradient	$\frac{\mathrm{m}}{\mathrm{s}}, \frac{\mathrm{ft}}{\mathrm{min}}$
T_{max}	maximum thrust	N
T_{req}	required thrust	N
k_{Prop}	ratio between propeller pitch to diameter	$-$
D_{prop}	diameter propeller	m
η_{Prop}	propeller efficiency	$-$
n_{RPM}	rotation speed	$\frac{1}{s}, \frac{1}{\mathrm{min}}$
n_{prop}	number of propellers	$-$
F, T	thrust force	N
p_{prop}	propeller pitch	m
D	drag force	N
P	power installed	W
R_{max}	maximum range	km
v_{Rmax}	speed for maximum range	$\frac{\mathrm{m}}{\mathrm{s}}$
h_{Box}	box height	m
m_{Tank}	tank weight	kg
m_{H2}	hydrogen weight	kg
m_{O2}	oxygen weight	kg
δ	wall thickness	m
δ_l	wall thickness for longitudinal stress	m
δ_t	wall thickness for tangential stress	m
σ_l	tension longitudinal stress	MPa
σ_t	tension tangential stress	MPa
σ_{zul}	permissible tension stress	MPa
R	gas constant	$\frac{\mathrm{J}}{\mathrm{kg\,K}}$
p	pressure	bar
$LxBxH$	length-beam-height	$\mathrm{m} - \mathrm{m} - \mathrm{m}$
Q	energy capacity	kWh
t	flight time	min, h
ΔC_P	pressure difference	$-$
$p(x)$	local pressure	Pa
p_∞	environmental pressure	Pa
$\alpha_{max,profile}$	maximum angle of attack of the airfoil	$°, \mathrm{rad}$
α_{max}	maximum angle of attack of the aircraft	$°, \mathrm{rad}$

List of Figures

List of Tables

1 Introduction

Everything from entertainment to the stock market, from maintaining a friendship to communicating with those friends in case of an emergency are dependent on the internet functioning perfectly. Thus, in our modern society the ability to have a connection to the outer world is of critical importance. However, when land bound connections fail due to a disaster, we are all at our most vulnerable. Quick and accurate communications between the victims of a disaster and their rescuers is lifesaving. To counteract such a critical failure of our communication systems, *AirLive*, as system out of *AirShip's*, seeks to provide temporary relief during disasters until land-based internet can be reestablished.

Flying at high altitudes for long durations is a profound challenge that in the history of mankind has only been recently unlocked. The invention of lightweight electrical motors, new hydrogen fuel cells and battery technologies have made this achievement possible. Thus, a relatively cheap and small plane to cover a large area for a long period of time can be realised. *AirLive* seeks to exploit these technologies in order to make an emergency internet connection possible.

In this report we will present a design proposal for an aircraft that flies at such altitudes and that can carry the weight of the modules necessary for it to provide internet coverage during emergencies. It also discusses the possible ways of covering an area where the internet went down.

2 Market Analysis

Due to global warming, the number of severe natural disasters is increasing. In 2022, there were over 420. [1] The number will be drastically higher in 2040 and beyond. These large numbers create a great need for rapid aerial reconnaissance and thus a very large market that we can serve.

In order to get an initial design idea, we had a look at the current situation of emergency communication aircraft. The most promising type of aircraft are high altitude flying platform stations (HAPS) defined by the International Telecommunication Center as "a station located on an object at an altitude of 20 to 50 km and at a specified, nominal, fixed point relative to the Earth." Due to their high altitude and long endurance these aircraft are capable to observe and communicate like satellites. At the moment there are several design projects and prototypes being developed:

Airbus Zephyr – Expecting to entry into service by the end of 2024, the Airbus Zephyr project will be one of the first non-military used HAPS to enter commercial production. It is a solar powered UAV known for its long endurance, currently up to 64 days. About 1000 aircraft are anticipated to fly within a 10-year period, providing up to 2.9 billion people with mobile service as well as emergency 4G/5G coverage. [2]

HAP alpha – Being developed by DLR the HAP alpha project is a full-scale technology demonstrator for high altitudes. It is designed to operate payload systems at an altitude of 20 km. The lightweight UAV aircraft is not supposed to be a commercial product, but to be a testbed for various technologies like solar panels. The first flight is expected in 2024. [3]

StratoStreamer – Powered by a hydrogen fuel cell propulsion the StratoStreamer is a UAV high flying platform developed by Leichtwerk AG at the Braunschweig research airport. The payload of the aircraft is specialized for sub-6-GHz mobile communication. [4]

RQ-4 Global Hawk – Even military aircraft can have a similar use case. The Global Hawk as a High-Altitude Long Endurance (HALE) aircraft with an endurance of up to 30+ hours and a service ceiling of 60000 ft (18.29 km) can also be used for communication coverage. [5]

Satellites – Currently, all available satellite-system for internet are privately hold by companies, like STARLINK. But to receive mobile service from space one needs an antenna on ground, which is not an option for us.

3 Assumptions

Before we started the design process, we discussed important assumptions to fulfil the requirements as best as possible. This determines how we design our aircraft.

CS-Aerodromes B1 – Our goal is to operate from as many aerodromes as possible, while not interfering with conventional air traffic. Therefore, we analysed all certified airfields in Germany. With a wingspan limitation of less than 24 m and a total aeroplane reference field lengths of under 800 m we can operate from almost all 434 aerodromes in Germany.

The aeroplane reference field lengths are categorised by the EASA in 4 groups and we counted the number of aerodromes we could serve from.

Table 3-1 CS-Aerodromes Aeroplane reference field length

Code number	**Aeroplane reference field length**	**Number of Aerodromes in Germany (434 in total)** [6]
1	Less than 800 m	199
2	800 m up to but not including 1200 m	146
3	1200 up to but not including 1800 m	47
4	1800 m and over	42

One of our own requirements is the ability to take-off and land on several runway surfaces, like asphalt, gras or gravel.

Winch launch system – This way we are able to reduce the take-off distance. In addition, we have more freedom in positioning the propellers at the wings.

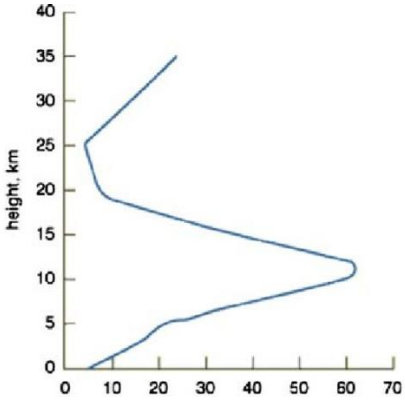

Fig. 3-1 Average wind speeds in different altitudes [48]

Flight altitude of 20 km (FL656) – We defined a flight level for our missions, considering conventional air traffic, wind speeds and humidity in the stratosphere, the international standard atmosphere and the potential area covert with internet by one aircraft. The weather plays a major role during climb and descent as it could be potentially dangerous to fly in very humid conditions, rain, icing or lightning. The uncontrolled air space starts at FL 660 in Europe and FL600 in USA. Although the plane still flies in regulated airspace, most civilian aircraft fly no higher than FL400, so our aircraft is unlikely to interfere with them.

Another point of consideration was the air temperature of 216.65 K for the thermal management and the density of 0.0879 kg/m³ for the propulsion system.

Cruise Speed – As required in mission 2, we need to fly 170 nm in less than 2 hours, which means a minimum ground speed of 43.73 m/s. As we can see in the following Fig. 3-2, the average wind speed at 20 km altitude is almost minimal with less than 10 m/s. Hence, we chose a first design cruising speed of 55 m/s for our aircraft, considering gusts, wind and mission 2.

Container –They make transportation easier, faster and cheaper since almost all companies adopted that system. Commonly used in commercial transportation are standard shipping containers, called TEU and FEU.

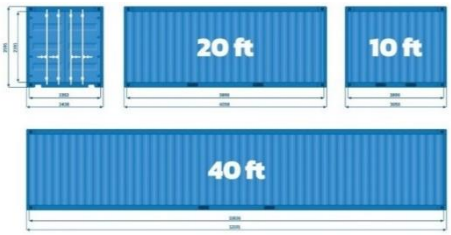

Fig. 3-2 Standard Container [7]

Table 3-2 Standard Container [8]

Container Standard	20 ft (TEU)	40 ft (FEU)
LxBxH (Interior) [m]	5.896x2.274x2.34	12.032x2.274x2.34
Max Payload Weight [kg]	28310 (28200)	26730 (28800)
Door Height [m]	2.339	2.340

4 Aircraft Design: *AirShip-E216*

For our aircraft design we discussed different configurations. First, we thought about designing a Zeppelin due to its low energy demand while hovering over a specific location. Unfortunately, they cannot keep up the speed required in Mission 2 and they cannot fly at high altitudes, which would have required many Zeppelins to operate during an emergency.

Secondly, we talked about a dragon configuration, which is well researched. [9] In order to fly at 20 km we would need a high wingspan for aerodynamic performance, but due to our restriction to operate from small aerodromes we just have a limited wingspan available. Thus, this configuration was not optimal for our purposes.

Furthermore, we thought about a blended wing configuration, which has a high aerodynamic efficiency. The disadvantage for our purpose hereby was the enormous chord, because we would have not been able to store it in standard containers.

Taking into account all restrictions, we chose a box wing configuration with a decent wing area and great aerodynamic performance, while keeping the total beam limited to 24 m and the chord smaller than 2 m.
From this point on we define the wing in front as “Wing 1” and the rear wing as “Wing 2”.

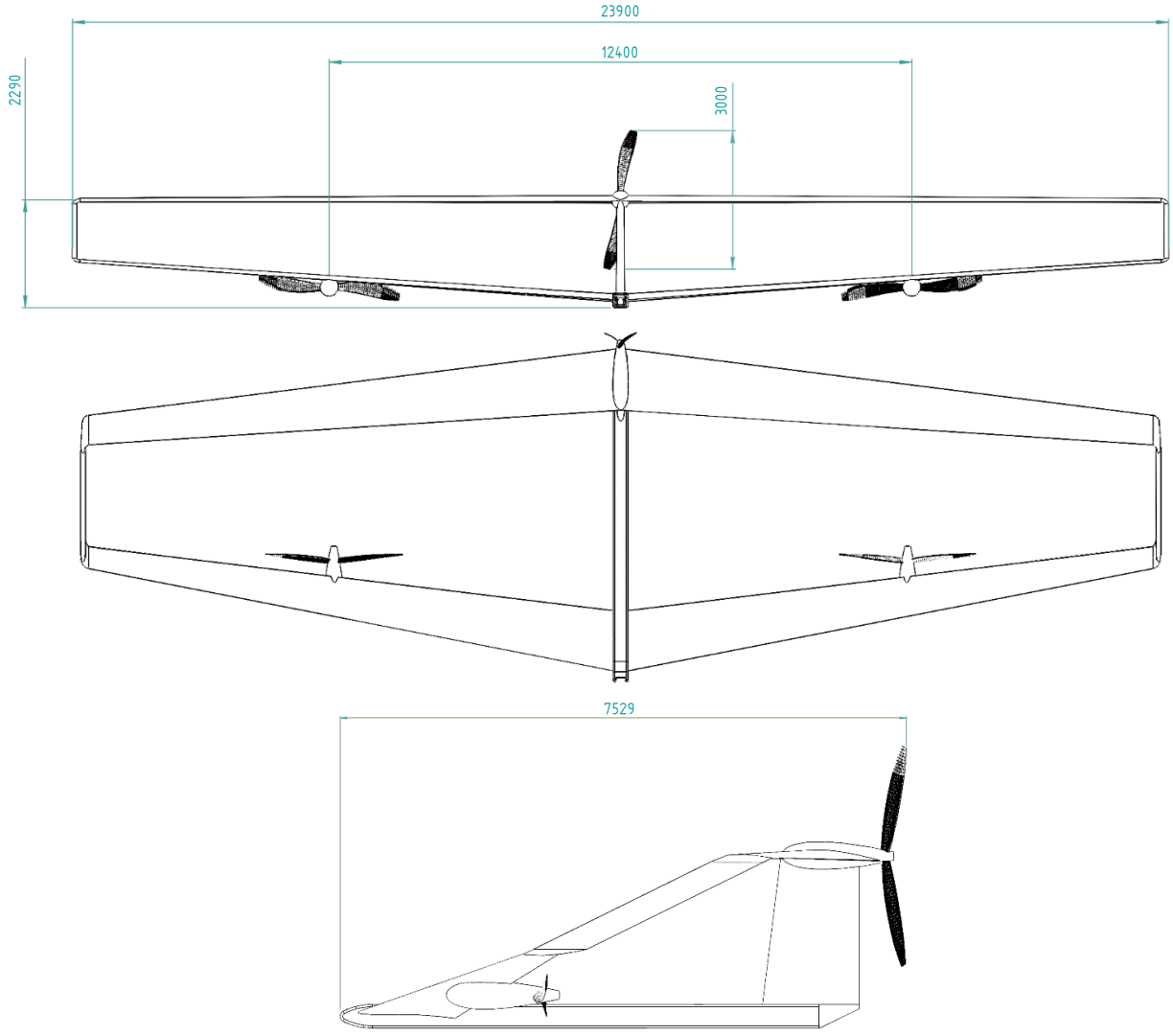

Fig. 4-1 *AirShip-E216* - 3 side view

Box – The boxes connecting the wing tips is our main aerodynamic feature for efficiency and stiffness. We decided on sharper corners at the joints to make them cheaper to produce than a completely round shape. Edgy boxes also fit better in the transport containers. The height and sweep are optimized to minimize the mass of the box in respect of its maximum efficiency. As the sweep increases, the mass increases because we need a greater chord to maintain stiffness against bending and shear forces. The height should be great enough that a human can walk under wing 2 while loading the aircraft, but also low enough to be in reach for maintenance. In addition, the box-module should fit in any orientation in a standard container. Regarding the aerodynamic efficiency of the box, the height-to-span ratio should be enlarged, as it would be best, but on the other hand increasing the mass at the wing tip. This results in a height under wing 2 of around 2.1 m.
Gear – Our main landing gear is positioned in the center of the plane. The nose gear is directly located under wing 1 taking the loads from the wing and transferring them into the ground. This minimizes the size and the mass of the stiff and heavy structure required. In addition, it is functioning as a hook for the winch launch.
The rear gear is for steering and transferring loads as well in the ground. It is located under the rudder bearing. The side gear is just for assistance to prevent wing strikes while landing with strong side gusts. They are in the pods of the engines at wing 1. The size itself is around 15cm in diameter similar to sailplanes, which will help the aircraft to roll on uneven grass runway. If necessary, a spring damper system could be installed as well.

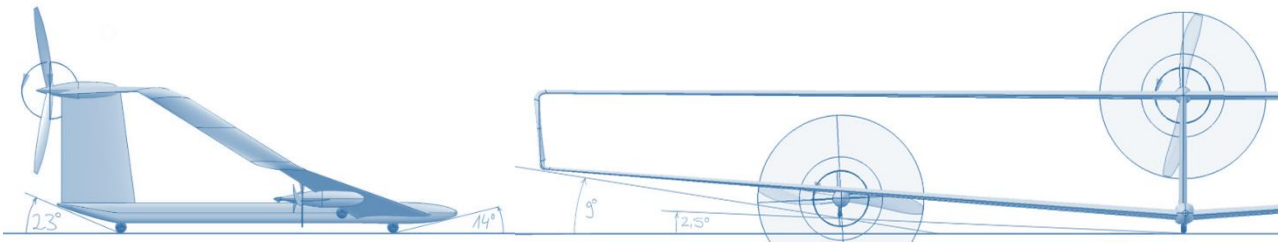

Fig. 4-2 Ground Clearance (propeller in horizontal position locked)

All gears are retractable to minimize drag. Every wheel is identical to minimize overall production costs.

Modularity – Our *AirShip-E216* is designed to be disassembled, meaning the possibility to exchange wings, fuselage or the box for other design layouts. Each wing will be split into two parts for transportation purposes. The connection is in the middle within the fuselage and the connector tubes absorbing the bending moments. If needed, the fuselage could be substituted for example by a larger one to fit more payload inside. The best part of this future cutting-edge technology is the ability to be used for other aircraft designs and a big aircraft family.

Propeller – We decided to go with 3 identical propellers with 2 blades each. Two are mounted at wing 1 and the third is at the top of the rudder mainly to guarantee stability with full thrust. Shortly before touchdown on landing, the two propellers on wing 1 are locked in a horizontal position to avoid damage. To fit them as close as possible to the trailing edge and the engine mount for a shorter shaft, we designed them with a pre-coned shape of 10° backwards to avoid damage to the wing. They are mounted at the trailing edge to provide a clean airflow for the wing, even though the propeller efficiency is slightly decreased. The position in y direction is defined by the side gear position to maintain a decent angle for ground clearance. (see chapter 4.3.4)

Power System – Our pressurized hydrogen tanks will be fitted into the wings. The fuel cell is installed under the connection of wing 1 in the fuselage. For sufficient hydrogen operation we also need a battery as buffer and a compressor to provide enough oxygen for the chemical reaction. All the three engines are fully electric and identical. (see chapter 4.3.2)

Avionics – The whole aircraft is equipped with conventional and advanced technology for the avionics, like advanced lidar sensors and a detect and avoiding system. This way we will be able to operate autonomously and remote controlled. (see chapter 4.5)

4.1 Weights

We have estimated the weights by considering current technologies and structures, while thinking about the future. As for every aircraft on the market it is one off our main goals to minimize the weight for maximum efficiency. The wings are playing a major role for weights regarding its size and functions. Therefore, we discussed different configurations for the wing cross sections. Our final choice is described in detail in the aeroelastic chapter **Error! Reference source not found.**.

Table 4-1 Weights and center of gravity

ID	Name	Weight [kg]	x_{CG} [m]	z_{CG} [m]
1	Propulsion system Center	9.0	6.55	2.20
2	Propulsion system Right	9.0	2.19	0.30
3	Propulsion system Left	9.0	2.19	0.30
4	Wing 1 (incl. tank)	148.7	1.10	0.35
5	Wing 2(incl. tank)	149.6	5.27	2.34
6	Empennage	20.1	4.78	0.85
7	Fuel Cell	5.0	0.70	0.00
8	Power System	37.5	1.12	0.10
9	Avionics	3.1	1.52	0.09
10	Payload	13.0	2.15	0.00
11	Fuselage	50.7	3.10	0.06
12	Hydrogen	21.4	3.26	1.32

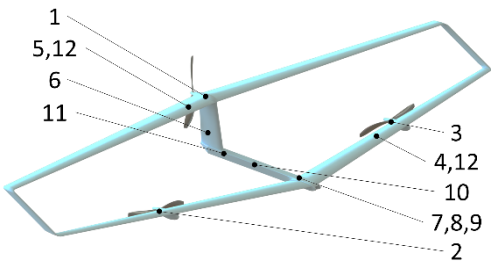

Fig. 4-3 *AirShip-E216* Components

That all sums up to a design take-off weight of $m_{TO} = 486\text{kg}$ and a maximum take-off-weight of $m_{TOmax} = 501\text{kg}$, which can be modified in future. The design center of gravity is at $x_{CG} = 2.90\text{m}$, $y_{CG} = 0\text{m}$ and $z_{CG} = 0.97\text{m}$. For stability we also computed the most aft CG $x_{CG,aft} = 3.14\text{m}$ limited by stability with a safety margin of 0. The most forward CG limited by trim capabilities, is much less critical for our design.
Design payloads are 1 radar module, 1 internet relay, a rot-antenna and an antenna system. Our maximum payload weight is 28 kg with 1 radar module with 5 kg, 4 internet relays with 5 kg, a rot-antenna with 1 kg and an antenna system with 2 kg resulting in $x_{CG} = 2.93\text{m}$. The center of gravity for the payload can be adjusted be placing it at different positions. The rudder and boxes are part of the empennage. The power system consists of the battery as reserve, the pipes for the fuel cell and the compressor unit. Parts of the avionics are the lidar sensors, the camera, the flight computer, the aircraft radar system, a transponder, the detect and avoidance system, measurement systems and the lights.

4.2 Aerodynamics

Now, after specifying the requirements, the configuration and the weights, we started our research on the aerodynamics and performance by defining general specifications as following:

Table 4-2 General Specifications

Name	Symbol	Value	Unit
wingspan	*b*	23.5	m
wing area	*S*	41.24	m^2
design cruise speed	*v*	55	m/s
design Mach number	*Ma*	0.186	-
design cruise altitude	*h*	20	km
reference chord	*c*	0.924	m
aspect ratio	*AR*	13.39	-
power installed	*P*	30	kW

As one of the most important coefficients in aviation, the design lift coefficient results from the air density at 20 km altitude, the true air speed and the take-off weight:

$$C_L = \frac{2 \cdot m_{TO} \cdot g}{\rho \cdot v^2 \cdot S} = 0.87 \tag{1}$$

The wing shape was optimized to fit in a certain range of C_L and to keep the induced drag minimized.

4.2.1 Wing Geometry

As one can see, we have two wings, each with a relatively high aspect ratio for best aerodynamic performance. The mean aerodynamic chord for both wings vary slightly because of the different plan shape. This affects the stability as well as the different zero-lift coefficients because of the downwash-effect.

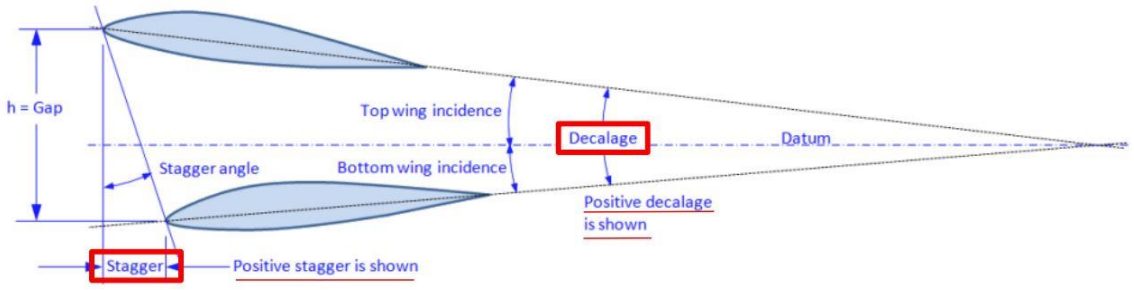

Fig. 4-4 General Wing Setup [10]

The stagger describes the horizontal distance between the leading edges of both wings at the root. The drag is independent from it. Researcher Scholz from the Hamburg University found that a stable box wing configuration requires a negative stagger and a higher lift coefficient for wing 1 [10].

A decalage, meaning the difference between the incidence angles of both wings, of 0° would be best for minimum drag in a conservative design. By changing the decalage one can counteract the downwash-effect from wing 1, but also decrease the maximum lift coefficient due to airflow separation.
We have defined our wing geometries separately to the following:

Table 4-3 Wing Configuration

Name	Symbol	Wing 1	Wing 2	Rudder	Unit
Chord Root	c_r	1.300	1.132	1.300	m
Chord Tip	c_t	0.455	0.623	1.038	m
Mean Aerodynamic Chord	c_{mi}	0.945	0.902	1.174	m
Taper ratio	λ_i	0.35	0.55	0.80	-
Sweep c/4	$\varphi_{25,i}$	10	-5	6.8	°
Twist	ϵ	2.5	2.5	0	°
Incidence Angle	θ	3	3	0	°
Dihedral angle	ψ	4	0	0	°
Zero-Lift coefficient	C_{L0}	1.005	0.732	0	-
C_{Lalpha}	$C_{L\alpha,i}$	5.841	5.906	2.300	-
Area	S	20.62	20.62	2.30	m^2
Aspect ratio	AR	26.78	26.78	1.69	
Aerodynamic Center	x_{25}	1.195	5.318	5.788	m
Aerodynamic Center	y_{25}	4.932	5.306	0	m
Aerodynamic Center	z_{25}	0.394	2.239	0.948	m

The total wing area S, the total aspect ratio AR and the reference chord c of the entire aircraft are then defined by the following equations. [11]

$$S = S_1 + S_2 \qquad AR = \frac{b^2}{S} \qquad c = c_{ref} = \frac{c_{m1} \cdot S_1 + c_{m2} \cdot S_2}{S} \tag{2}$$

In addition, we calculated the lift curve slopes to get a feeling for the change in lift by altering the angle of attack:

$$C_{L\alpha,i} = \frac{2 \cdot \pi \cdot AR_i}{2 + \sqrt{{AR_i}^2 \cdot \left(1 + \tan\left(\varphi_{25,i}\right)^2 - Ma^2\right) + 4}} \tag{3}$$

Dihedral – This angle is important for safety regarding lateral stability by resisting rolling and ground clearance (Fig. 4-2) to avoid wing strikes due to high bank angle resulting from side gusts.
Incidence angle – It is mainly to provide a sufficient lift coefficient in horizontal flight. By increasing this angle, the maximum AoA we can fly at decreases due to the maximum AoA of the airfoil.
Twist – Hereby we can adjust the lift distribution and stall characteristics of the whole wing. It is beneficial not to stall at the same time over the whole span. Its preferable that the wingtips with the ailerons stall later than the middle of the wing to maintain control of the plane.

4.2.2 Airfoil selection

An important part of an aircraft is the airfoil. Therefore, we computed our Reynolds number at the reference chord to 316’346. Then, we compared different types of airfoils, starting with the well-known Clark-Y. Unfortunately, it does not provide a sufficient lift coefficient, while having a relatively high drag coefficient in comparison to other airfoils, like the NACA 6412. This one seemed to be better for our application, regarding the low drag coefficient, but it could not keep up with the Eppler E216, optimized for small Reynolds numbers.

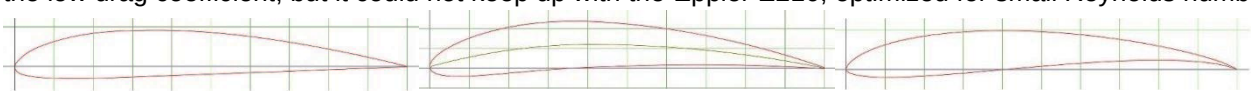

Fig. 4-5 Clark-Y, NACA 6412, E216 [12] [13] [14]

With the best lift to drag ratio at and the highest lift coefficient, we chose the E216. Nevertheless, we have to mention that the moment coefficient is quite high, as will be explained further in the chapter stability.

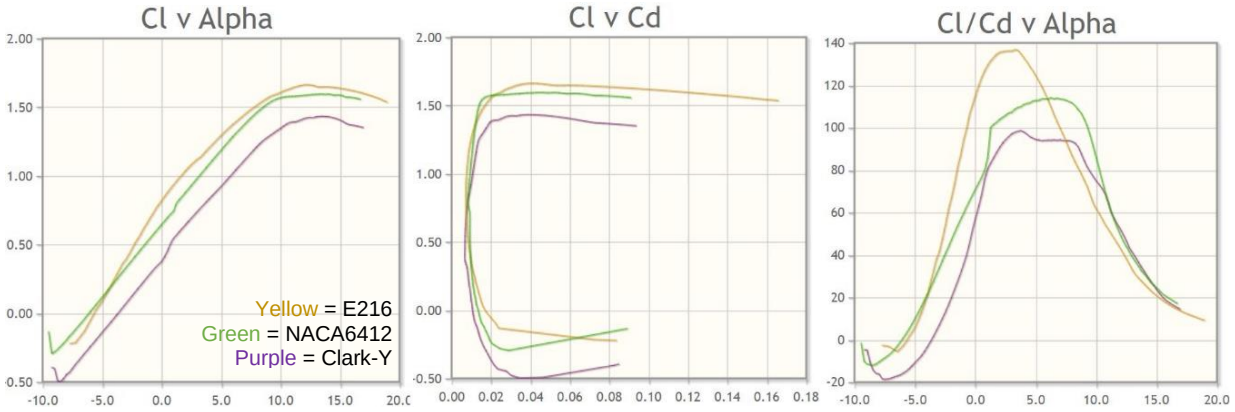

Fig. 4-6 Airfoil Polars Comparison (yellow=E216, green=NACA6414, purple=Clark-Y) [12] [13] [14]

Another aspect of the airfoil selection was the minimum thickness of ratio of above 10% to fit the hydrogen tanks inside the wings. The E216 airfoil has a relative thickness of 10.4%.

As part of the detailed design process, research could be done on a customised airfoil for further performance improvements, but this would quickly inflate the cost of the project.

4.2.3 Drag Coefficient

Zero-drag coefficient – We estimated this coefficient with hand calculations from material provided by the lectures of the ILR of the TU Dresden and verified them using VLM Software "OpenVSP". [15]

Table 4-4 Zero-drag coefficients

Name	$C_{D0,i}$
wing 1	0.00738
wing 2	0.00746
rudder	0.00095
box	0.00033
fuselage	0.00075

$$C_{D0} = \frac{1}{S}\sum_{k}\left[c_f k_F\, k_i\, S_{wet}\right]_k + \sum_{n}\left[\Delta C_{D0}\right]_n \tag{4}$$

$$c_f = \frac{0.455}{(\lg(Re))^{2.58}(1 + 0.144\, Ma^2)^{0.65}} \tag{5}$$

We assumed a turbulent boundary layer on all surfaces. The wave drag is negligible because our Mach number is always smaller than 0.3. This is the case because of its high efficiency while flying slow and because of the available limited thrust. In addition, we added several safety factors for the zero-drag coefficients, in example additional 3% on the total aircraft, 7% on the fuselage, 6% on the wings and 7% on the rudder.

Table 4-5 Drag Coefficients (Cruise Condition)

Name	Symbol	Value
Zero-drag coefficient	C_{D0}	0.0182
Induced drag coefficient	C_{Di}	0.0173
Total drag coefficient	C_D	0.0355

Induced drag coefficient – Due to our box wing configuration, it is difficult to compute the exact induced drag coefficient. In general, you can approximate it with the familiar formular for conventional aircraft.

$$C_{Di} = kC_L^2 = \frac{1}{e\,\pi\,AR}C_L^2 \tag{6}$$

In reality, the boxes counteract the vortices generated by the pressure difference between the upper and lower wing side reducing the induced drag. That is a reason why the boxes need a chord greater than 0, meaning a direct connection of both wing tips.

Sharkskin – The "AeroShark" technology for aircraft was invented by Lufthansa Technik [16] to reduce the drag by approximately 1%. Regarding our operational concept, we will only offer it as an option for our customers, because the fragility and the costs are not worth the advantage.

De-Icing – We will have no active de-icing system installed on our current design due to its extra weight. In addition, the humidity at 20 km is 0%, which means that the only critical part of the flight is climbing and descending through clouds. In winter, we plan to spray the aircraft with an environmentally friendly, aircraft de-icing fluid (ADF) just prior to departure. We might need some research on modified or new ADF, because there have been concerns raised about pollution of the groundwater.
Nevertheless, for further developments of the wings an active de-icing system, like heating wires in the skin should be considered.

4.2.4 Efficiency

For a boxwing configuration we found some information on the most efficient lift distribution:

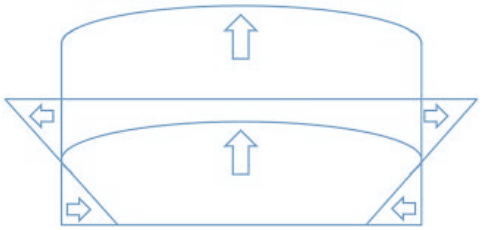

Fig. 4-7 Ideal lift distribution [17]

Table 4-6 Efficiency in numbers

Name	Symbol	Value
Oswald efficiency factor	e	1.033
Lift Curve Slope	$C_{L\alpha}$	5.049
Glid number	E	24.44
Maximum Glid number	E_{max}	24.45

By generating lift to inside at the bottom of the box and lift to the outside at the top of the box, the vortices can be reduced dramatically (Fig. 4-13).
Oswald efficiency factor – The high value of this factor in comparison to conventional aircraft is one of the main reason for a boxwing configuration. For Prandtl's best wing system is a vertical aspect ratio $V_V = \frac{h_{Box}}{b} = 0.09$ commonly used as part of the span-efficiency factor. Our value for **e of 1.033** was determined using OpenVSP and can also be found for other box wing configurations. Nevertheless, it still needs further research in detailed design to optimize the glide number.

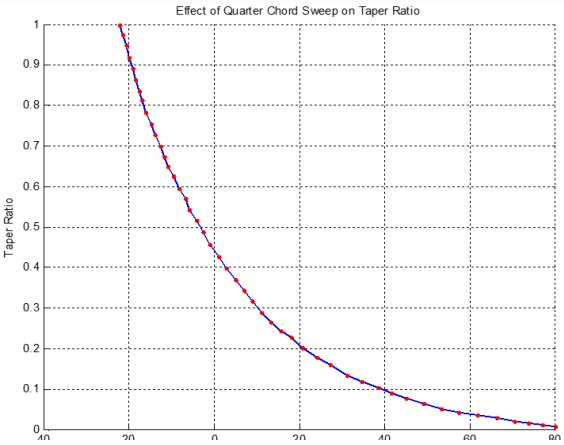

Fig. 4-8 Effect of Quarter Chord Sweep on Taper Ratio [18] [49]

As one can see in Fig. 4-8 for a non-twisted wing, an elliptical lift distribution also depends on the sweep. The blue line shows the combination of sweep and taper ratio for an elliptical lift distribution.
We need a decent sweep for a horizontal distance between both wings and fuselage length for sufficient longitudinal stability. A box with a higher sweep would have been heavier and result from a smaller sweep of the wings. Another point of attention is the vertical stability (see 4.2.5 Stability).
For the efficiency optimization we kept a fixed sweep and its relating optimal taper ratio and varied the twist. We decided to fly with a little twist to improve the assumed stall behaviours. For wing 1, we had to adjust the taper ratio from 0.3 to 0.35 to get a certain volume and height inside for tanks and to improve the stiffness.

Gliding number – As we want to fly as long as possible, this ratio between lift and drag must be maximized for cruise. Our plane needs to fly at an altitude of 20 km for maximum range at a speed of 54.38 m/s, which is almost identical to our design speed.

$$v_{Rmax} = \sqrt{\frac{2 \cdot m_{TO} \cdot g}{\rho \cdot S}} \sqrt{\frac{k}{C_{D0}}} \tag{7}$$

For maximum endurance we would need a true airspeed of 41.3 m/s, but due to our higher stall speed of 42.1 m/s (eq. (**20**), we can just fly as slow as possible. The value for 41.3 m/s results from the linear lift theory, which does not include any characteristics near stalling. That is why we need to adjust the minimum air speed for maximum endurance and define $v_{min} \approx 1.1 \cdot v_{stall}$.

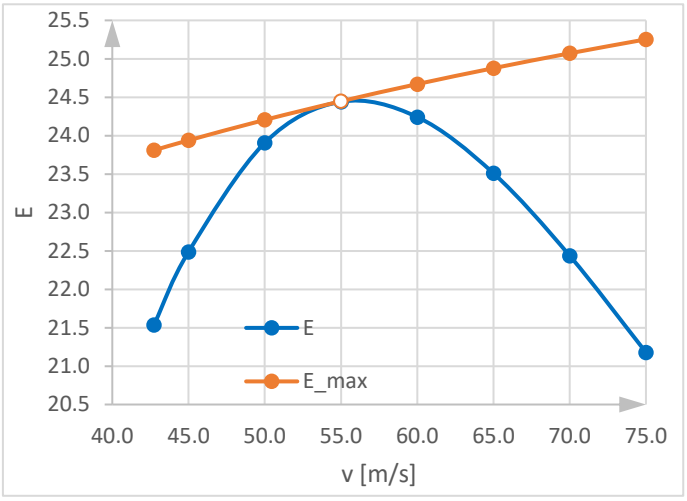

Fig. 4-9 Gliding number and speed

Maximal gliding number – Flying at the maximum gliding number gives us the maximum range. It can be computed with the formula:

$$E_{max} = \sqrt{\frac{1}{4\,k\,C_{D0}}} \tag{8}$$

resulting in a value of **24.45** for the design point. The result shows us, that our aircraft is most efficient at around 55 m/s for the missions as our cruise gliding number matches the maximum. Alternatively, we need to adjust the air speed for best performance.

The slight changes in the maximum gliding number results from the changing zero drag coefficient, as it is a function of the Reynolds number in the friction coefficient (**5**).

Downwash effect – It describes the change in angle of attack for wing 2 due to the aerodynamic actions by the airfoil of wing 1. This complex phenomenon plays a major role in stability and efficiency. We used an empirical formula for conventional aircraft as first estimation. Please note, that the distance between both wings changes due to their sweep angle. In this formula, the relative vertical distance is also not considered as a parameter.

$$\left(1-\frac{\partial\varepsilon}{\partial\alpha}\right)=\frac{\sqrt{4+AR_1^2\left(\frac{1}{\cos^2(\varphi_1)}-Ma^2\right)}-2-\frac{1}{2\xi^2}\left(\frac{1}{\cos^2(\varphi_1)}-Ma^2\right)}{2+\sqrt{4+AR_1^2\left(\frac{1}{\cos^2(\varphi_1)}-Ma^2\right)}}=0.721 \tag{9}$$

$$with\ \xi=\frac{x}{\frac{b}{2}}=\frac{x_{25.2}-x_{25.1}}{\frac{b}{2}}=0.239 \tag{10}$$

The upwash induced by wing 2 is negligible as we have a negative stagger.

Lift Curve Slope – The theoretical maximum for our wings as a plate would be 6.395. By substituting $2\pi AR$ in equation (3) with $0.9\cdot C_{L\alpha,profile}$ for a airfoil, we get 5.678. But we have to consider the downwash effect leading us to the modified equation (11) [18]

$$C_{L\alpha}=C_{L\alpha1}\frac{S_1}{S}+C_{L\alpha2}\frac{S_2}{S}\left(1-\frac{\partial\varepsilon}{\partial\alpha}\right)=5.049\frac{1}{\text{rad}} \tag{11}$$

Flaps – We do not use high lift devices like slats or flaps because our high wing area S provides enough lift in any condition. One advantage of not having flaps is the lower weight of the entire aircraft. In addition, we are far less vulnerable to failures or malfunctions of such a complex system, which is an advantage during an emergency operation.

Ailerons – We plan to install just two ailerons at wing 2 to reduce costs and weight. They will be sufficient for turning and functions as elevator simultaneously.

Nose up trim | Left turn trim | Nose down trim

Fig. 4-10 Trim in frontal view on aircraft (presentation not to scale)

By deflecting both ailerons upwards, our aircraft will increase the AoA, due to the reduced lift on wing 2. The opposite is true for a downward deflection. Note that in a turning flight a correction with the rudder is required to continue horizontal flight as the ailerons are behind the center of gravity. For other wing configurations a different wing 1 with ailerons could be installed, as the whole aircraft is modular, if more controllability and redundancy is required. In this case it would be possible to deflect both ailerons downward to function as flaps.

Morphing wing – This future technology decreases the drag coefficient by eliminating the split between the main wing and the ailerons or rudder, as demonstrated on a Gulfstream III by NASA and the US Air Force. [19] Our aircraft will profit from this with the two ailerons and the rudder.

Service Ceiling – It describes the altitude at which we can fly and climb even at 100 ft/min with a maximum Mach number of 0.3. Its limitation are the engine power, the maximum lift coefficient and the maximum Mach number. We have included a propeller efficiency of approximately 80% in this calculation.

$$T_{max} = \frac{P_{max}}{v} = \eta_{prop}\, m_{TO} g \left(\frac{C_{D0} + k\, C_L(\rho)^2}{C_L(\rho)} + \frac{\gamma}{a(\rho) \cdot Ma_{max}} \right) \quad with \quad \gamma = 100 \frac{ft}{min} = 0.508 \frac{m}{s} \tag{12}$$

After computing the air density at the service ceiling to 0.0231 kg/m³, we can say that an altitude of **28.4 km** could be flown with 25.46 kW power (incl. climbing) and C_L=1.227<$C_{L,max}$. We cannot fly at full power, otherwise the maximum Mach number is exceeded, which is limited by the propeller.

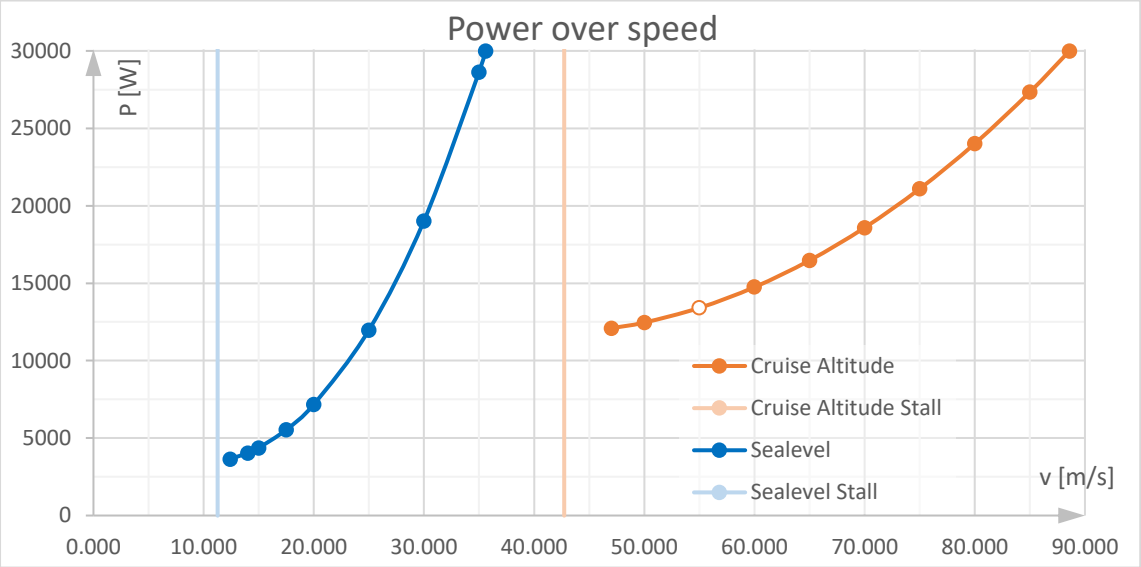

Fig. 4-11 Power required from v_{min} to v_{max}(P_{max}) at different altitudes

Our design point is displayed as white dot. The Fig. 4-11 was created with the design payload, as described in 4.1 Weights. If we are interested in the maximum flight endurance, we should fly as low and as slow as possible.

Table 4-7 Performance at different altitudes

h [m]	v_{stall} [m/s] at C_{Lmax}	v_{min} [m/s]	v_{max} [m/s] at P_{max}=30kW	P_{min} [W] at v_{min}
0	11.28	12.41	35.95	3695
20000	42.10	46.31	88.44	12118
28400	82.14	90.35	90.34*	25456

* P_{max} is not reached due to Ma_{max}

For cruise altitude at design speed we get the following polars:

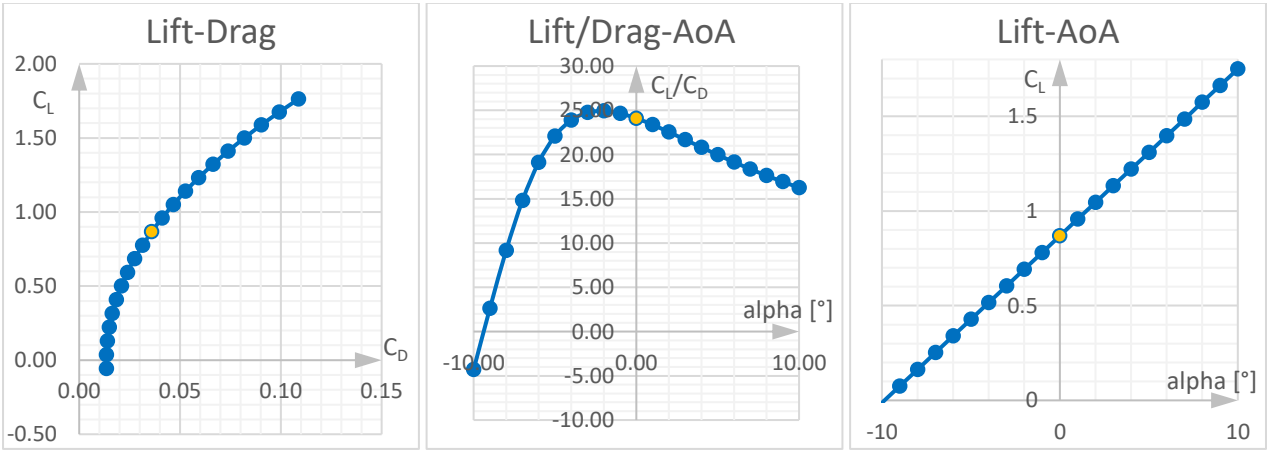

Fig. 4-12 *AirShip-E216* Polars and Performance (*h*=20km, *v*=55m/s)

Regarding the lift-AoA diagram one must know that we do not display any stall characteristics. The yellow dot in the lift-drag-diagram shows the ratio for an AoA of 0°. As one can see, the highest glide number can be achieved at an AoA of -2°.
Running some computation with OpenVSP gives us the pressure distribution.

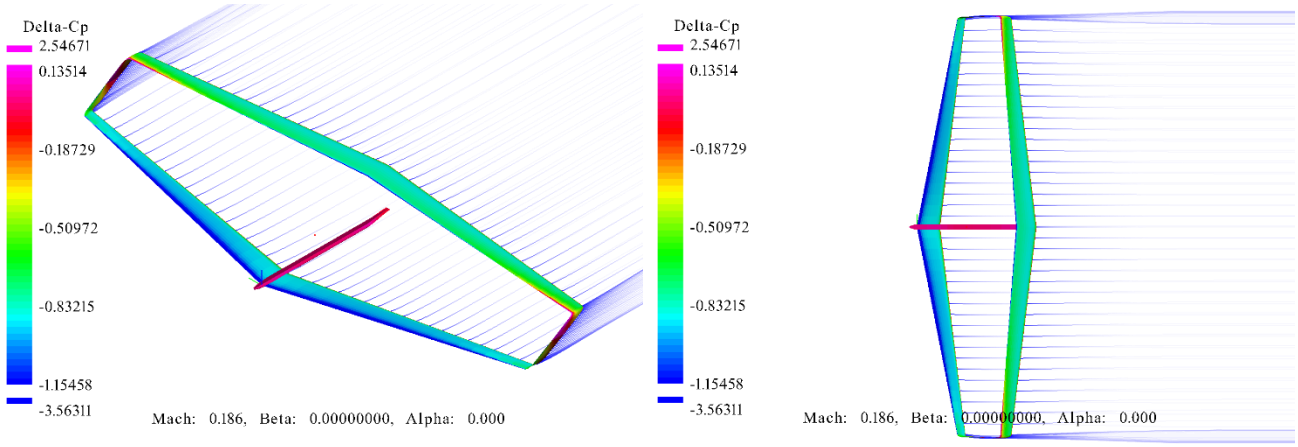

Fig. 4-13 Aircraft local pressure coefficient differences

In Fig. 4-13 the delta of the pressure coefficient ($\Delta C_p = \frac{p(x)-p_\infty}{\rho/2 \cdot v^2}$) is shown with the simplifications of neglecting the engine pods and rudder as they would affects the colour grading. One can see that wing 1 has a significantly higher ΔC_P value than wing 2, which can be related to the downwash effect in (**9**). The box sees a strongly varying ΔC_P. In the top view are the counteracting vortexes of the boxes visible, which will give us superior efficiency. These calculations were run to verify our hand calculations.

4.2.5 Stability

Longitudinal static stability – As one of the most important characteristics of an aircraft for flight performance and safety we took a deeper look at the longitudinal stability, especially for our high aspect ratio wings and the relatively short fuselage. There are different approaches for a box wing configuration, so we decided to compute the neutral point with a basic moment equilibrium about center of gravity with the mean aerodynamic chords. Assuming *T*<<*L*, we simplified the equation by neglecting the thrust

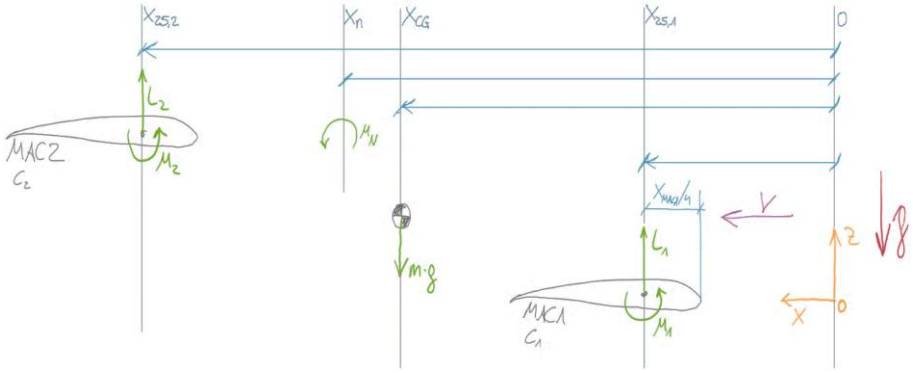

Fig. 4-14 Longitudinal Static Stability

$$M_{CG} + M_1 + M_2 - L_2(x_{25,2} - x_{CG}) + L_1(x_{CG} - x_{25,1}) = 0 \tag{13}$$

With the general moment coefficient, we transformed this equation to receive C_{MCG}. Other terms in the moment coefficient are negligible. Note, that *q* defines the dynamic pressure and *n* the load factor.

$$C_M = \frac{nM}{qSc} = C_{M0,i} + C_{M\alpha,i}\alpha \quad and \quad C_{L,i} = C_{L0,i} + C_{L\alpha,i}\alpha \quad |i = 1,2 \tag{14}$$

$$with \quad C_{L0,i} = \frac{C_{L\alpha,i}}{C_{L\alpha}} C_L \left(1 - \frac{\partial \varepsilon}{\partial \alpha}\right) \quad and \quad C_{M\alpha,i} = C_{L\alpha,i} \cdot c_{mi} \quad |i = 1,2 \tag{15}$$

A value for $C_{M0} = -0.2$ can be seen in the airfoil polars. (Fig. 4-6)

The zero-lift coefficient of each wing depends on the downwash-effect. Note that $\left(1-\frac{\partial\varepsilon}{\partial\alpha}\right)=1$ for wing 1 as it is not affected due to its free flow, while wing 2 is affected by wing 1.

$$C_{MCG}=\frac{S_1}{S}\frac{C_{L1}}{c}\left(x_{25,1}-x_{CG}\right)+\frac{S_2}{S}\frac{C_{L2}}{c}\left(x_{25,2}-x_{CG}\right)-\frac{S_1}{S}\frac{c_1}{c}C_{M2}-\frac{S_2}{S}\frac{c_2}{c}C_{M2} \tag{16}$$

Now, we were able to separate terms depending on alpha and terms not depending on alpha to compute $C_{M0}=0.22$, which must be greater than 0 and $C_{M\alpha}=-3.19\frac{1}{\mathrm{rad}}$, which must be smaller than 0 for static stability. To receive a valid neutral point, we computed the moment equilibrium about the neutral point with x_N as variable.

$$M_N-L_1\left(x_{25,1}-x_N\right)-L_2\left(x_{25,2}-x_N\right)+M_1+M_2-mg(x_N-x_{CG})=0 \tag{17}$$

Per definition of this point the moment is either 0 or constant.
Fill this equation with coefficients and reorder it for x_N and divide every term through the mass m_{TO} and g.

$$x_N=\frac{C_{L2}S_2x_{25,2}+C_{L1}S_1x_{25,1}-C_{M1}S_1c_1-C_{M2}S_2c_2-\frac{1}{q}x_{CG}}{C_{L1}S_1+C_{L2}S_2-\frac{1}{q}}=3.145m \tag{18}$$

Safety Margin – Must be greater than 0 for a static stable aircraft. But to reduce trim drag it should be as small as possible. The safety margin is defined with the relative length coordinates $h_i=\frac{x_i}{c}\ \ |i=CG,N$

$$SM=h_{CG}-h_N=0.230>0 \tag{19}$$

Our aircraft is longitudinal static stable. Due to our flexible loading system, we can modify the center of gravity before flight.
As a plausibility check we added to the counter of the fraction of eq.(**18**) $-ScC_{MCG}$, which gives us a safety margin of 0 as it is supposed to be.
Lateral and Vertical Static Stability – are fine. Due to the dihedral angle of wing 1 we will maintain lateral stable. The sweep angle creates different wind speeds during sideslip, which has the tendency to roll to wings levelled for a backward sweep. The opposite is true for a forward wing sweep. The boxes and rudder prevent a deep sideslip during turning flight with bank angle. In addition, they have a sufficient sized area of 2.3m² for the rudder and 1.8m² for both boxes for vertical stability, respectively yawing. In future developments, one must determine the precise Dutch roll characteristics. [20]
Stall characteristics – We determined the stall speed at 20 km of our aircraft to

$$v_{stall,TAS}=\sqrt{\frac{2W}{\rho SC_{Lmax}}}=42{,}73\frac{\mathrm{m}}{\mathrm{s}}\quad v_{stall,EAS}=11.45\frac{\mathrm{m}}{\mathrm{s}} \tag{20}$$

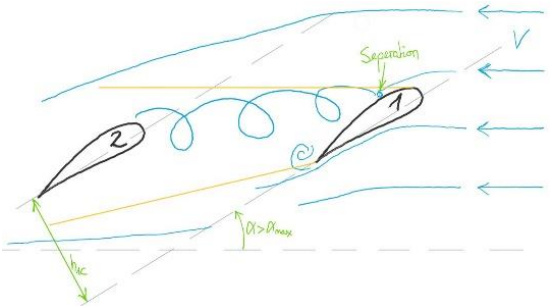

Fig. 4-15 Stall of a box-wing (schematic)

From the airfoil poles, we get the maximum AoA ($\alpha_{max,profile}\approx 12°$), from which the incidence angle must be subtracted, to receive the maximum AoA of our aircraft to $\alpha_{max}\approx 9°$. The critical point for this value is the wing 1, as the AoA of wing 2 is always smaller due to downwash. In turning flight, the stall speed increases, which grow the tendency to spin and unstable flight condition. The stall speed also rises during high G manoeuvres. Nevertheless, during stalling a nose down moment is beneficial to gain speed and thereby lift.
Normally wing 1 stall before wing 2 due to the downwash-effect. If in our case wing 1 begins to stall due to a high angle of attack, the turbulent airflow will also cause wing 2 to stall. the yellow lines schematically show the area of turbulent air flow. Important hereby is the vertical distance h_{AC} between both wings because the effect of the downwash decrease with an increasing h_{AC}.

4.2.6 Wing Loads

Starting this chapter, we determine the average wing loading to $\frac{W}{S} = 115.56 \frac{\mathrm{N}}{\mathrm{m}^2}$.In detailed design process you must always keep in mind the balance between aerodynamics, dynamics and elasticity.

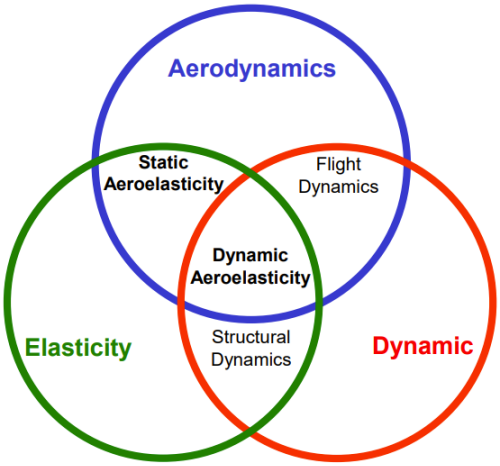

Fig. 4-16 Balance of Aeroelasticity

Wing Structure – The wing must be able to lift the weight of the entire aircraft in flight and at the same time support its own weight on the ground. These loads are mainly carried by the hydrogen tanks. They are connected to the main frame with connector-tubes. This layout saves weight by utilizing the existing tanks as structural elements, even if they are pressurized with hydrogen. In order to absorb the pressure loads, the fibres must be laminated at 0° for circumferential stresses and at 90° for longitudinal expansion. Due to the bending and twisting of the wing in flight, additional layers of 45° laminate will be required to compensate shear stresses. APUS as company proves that this concept is working with their hydrogen plane. [21] The skin of the wing is made from Carbon reinforced fibres. These CRFs are constructed with a sandwich structure of foam in between them.

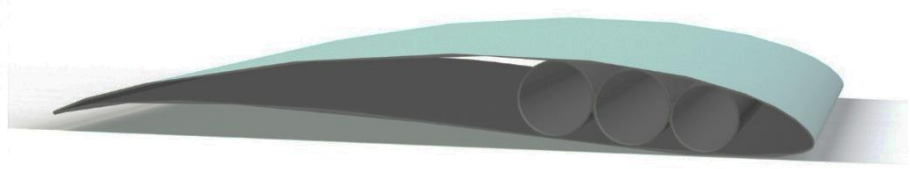

Fig. 4-17 Wing cross section

The box wing configuration has an additional advantage for the overall stiffness of the aircraft because of its framework. With respect to the aerodynamic efficiency the height of the box should be minimized. To optimize the box geometry a whole research study will be necessary during the detailed design process.
We computed the loads for the wings. A simplification is the negligence of the propulsion system in wing 1, the landing gear and the tanks including the hydrogen.

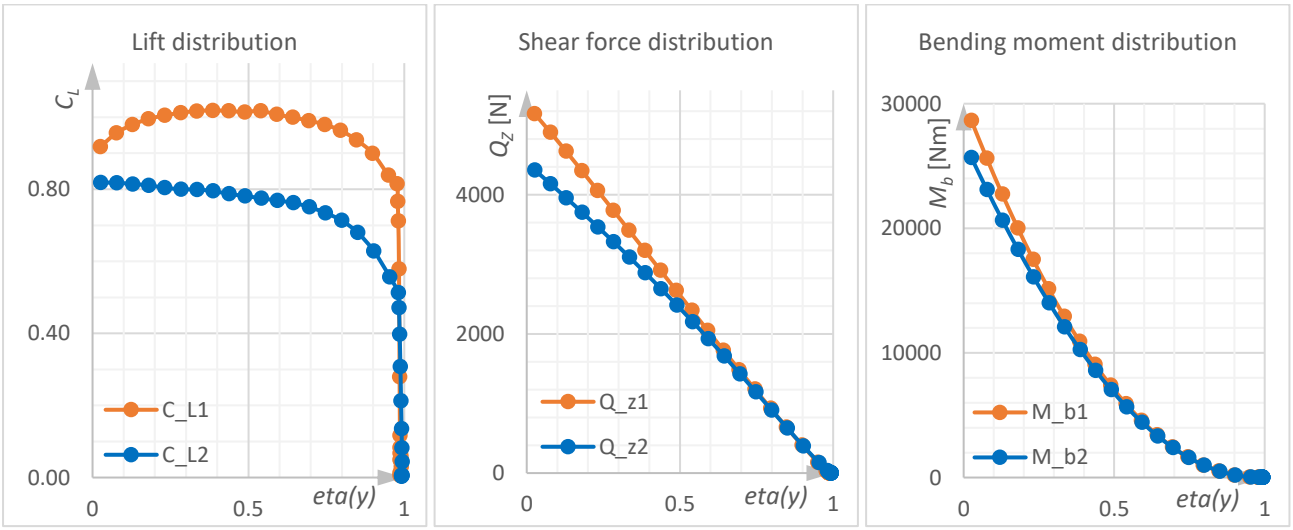

Fig. 4-18 Lift distribution, Shear Force, Bending Moment over normalised half wingspan (*n*=1 g) (orange=wing 2, blue=wing 1)

$$Q_{z1} = 5164.4\ \mathrm{N} \qquad Q_{z2} = 4355.8\ \mathrm{N} \qquad (21)$$
$$M_{b1} = 28648.6\ \mathrm{Nm} \qquad M_{b2} = 25675.4\ \mathrm{Nm}$$

One can see, there is a difference between the lift coefficient of the two wings, which attributes to the downwash-effect as described earlier in (**9**) and (**15**).
In (**21**) are the total values for shear forces and moment reaction in cruise configuration. Regarding the certification a maximum load factor must be defined.

Buffeting – The design critical phenomena occurs when the airflow separates and the wing loading oscillates along the chord. It is caused by the interaction of the aircraft with disturbed or uneven airflow, such as when flying through turbulent air or at high angles of attack. Buffeting can be a concern for aircraft because it can affect the handling characteristics and stability of the aircraft, as well as structural damage. To avoid that, a vortex generator might be installed or the wing shape might be slightly modified.
Special focus is necessary on the natural frequency of the boxwing configuration due to the connection and aerodynamic influence of both wings. A keyword in this topic is the “thumb print” criterion. [22]

4.3 Propulsion

One of the most important topics to think about when you start to design an aircraft is the way to provide the energy for flying. This of course includes the energy for the propulsion but also the energy for the flight computers, sensors, actuators and the payload and communication systems. First, we look at the more conventional solutions for this task. With the flight altitude at 20 km the density of the air is only 7% of the density at sea level. So, jet and combustion engines do not work efficiently at this altitude, especially with our low flight speed. Resulting from this assumption we believe that an electric powered propeller to be the best way to produce the thrust for our airplane. For the electric engines we looked at the best solution for our task, considering aspects like the power to weight ratio and reliability. Brushless DC motors are the best choice for this task with a possible power to weight ratio of 10 kW/kg and a long lifetime without maintenance because of the brushless design. The necessary power depends on how fast we want to climb to arrive at the location. We have chosen 30 kW for this task, the calculation with this number can be found in chapter 4.2.4 Efficiency.

4.3.1 Solar Cells

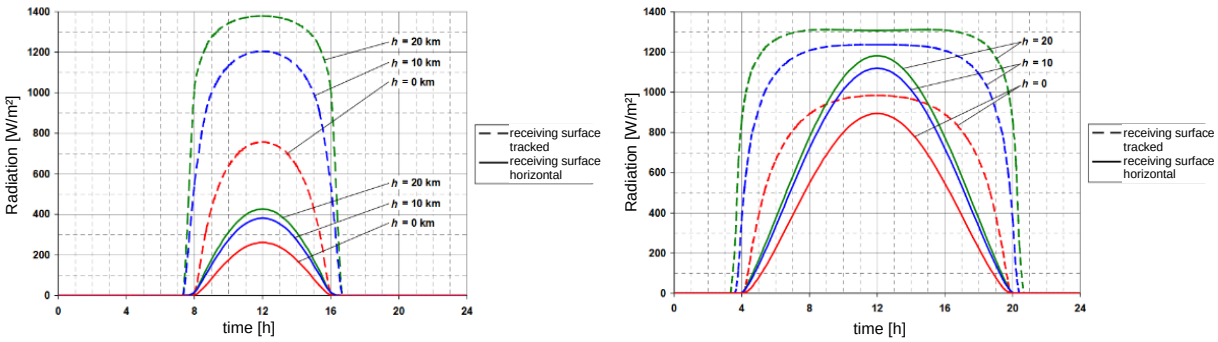

Fig. 4-19 Sun Intensity at 48°N (captions translated to English) [23]

Table 4-8 Power from sun in winter and summer

Average energy	$6.35\,\frac{\mathrm{kWh}}{\mathrm{d}*\mathrm{m}^2}$
Peak energy (summer)	$11.3\,\frac{\mathrm{kWh}}{\mathrm{d}*\mathrm{m}^2}$
Minimum energy (winter)	$1.4\,\frac{\mathrm{kWh}}{\mathrm{d}*\mathrm{m}^2}$
Total area for panels	40 m²

Table 4-9 Solar cell comparison [24] [25]

Type	**monocrystalline silicon** [26]	**CIGS thin-film modules** [27]	**Unit**
Total weight	32.6	120	kg
Efficiency	0.23	0.15	-
Average energy	58.38	38.1	kWh/d

CIGS thin-film modules are too heavy and thus require more energy than they deliver. The monocrystalline solar panels used on other solar aircraft would slightly be worth it from an energy perspective, especially in summer.

In winter they represent an additional weight. Unfortunately, these panels are very expensive and not very resistant to dirt and other extreme weather conditions. Since our aircraft are exposed to these influences every day, solar modules are not worthwhile for us. In addition, the handling during assembly and disassembly of our plug-in total concept is very complicated and requires expensive specialists. [28]

4.3.2 Storage System

So, we have selected the way to produce the thrust. Now we considered which kind of energy storage would be the best for our missions.

Jet Fuel – Fossil fuels are not an option for us because even in our scenarios, we want to use environment friendly propulsion systems for our airplane. Synthetic fuels are a better way to achieve an environment friendly propulsion system but we still have the problem with the low air density. So, a compressor or turbocharged internal combustion engine with an electric generator might be an option. But we need to consider the low efficiency at this altitude and the efficiency of the generator.

Radionuclide batteries – This kind of energy system provides the energy for years, so we don't need to refill the energy storages. But the downsides are the low efficiency which brings a low energy to weight ratio. But the bigger problem is the radiation. Keeping the handling a safe work for the ground crew would be a really challenging task. An accident with this kind of airplane can cause serious environmental damages and even the safety of people would be in danger. This results in the requirement of heavy safety measures. The cost for radioisotopes like plutonium is in the range of over 1mio$ per kg. There are way too many downsides for radionuclide batteries and even the possibility of flying non-stop is not worth it.

Batteries – The biggest advantage of using batteries at this altitude is that they don't need air. Batteries won't lose any efficiency at 20 km altitude. The major problem with batteries is the low energy density, which is mainly in focus as research topic all around the world. The increasing numbers of electric and hybrid cars are boosting this research. Regarding entry into service in 2040 a big increase in battery technology can be expected. Nevertheless, a big downside of batteries is the use of rare metals which produce big environmental damage at the mining. But we still need to look close at the future development of batteries.

Hydrogen – The last energy storage we considered is hydrogen with the use of a fuel cell to produce the electric energy. Hydrogen has a big advantage with a decent energy density of 33.3 kWh/kg. Fuel cells provide a great method to convert the chemical energy of Hydrogen to electric energy. With efficiencies of 60-70%, LT-PEMFC kind are a great choice for our airplane. Toyota is producing fuel cells with 2 kW/kg and 3.1 kW/l for the Toyota Mirai [29]. This means we need just a 15 kg fuel cell for our application. But even at sea level, these fuel cells need some kind of compressor to increase the air pressure. Flying the required oxygen with us is not in option regarding the heavy weight. At 20 km altitude we need some powerful compressor to deliver the pressure which is needed to run the fuel cell efficiently. The air inflow will be regulated by the rotational speed of the compressor. The biggest challenges for using Hydrogen are the storage of the Hydrogen and the cooling of the fuel cell. For storing hydrogen it's important to store it with high pressure because hydrogen is a gas with a very low density. An interesting way to store hydrogen in an airplane is to use cylindrical tanks for hydrogen but they are used as wing structure too. This reduces the extra weight we need for the high-pressure tanks. One research of APUS in collaboration with the TU Dresden is about this usage, it's called Apus i2 [30]. To estimate the weight of these tanks we used the equations for the stress in cylindrical pressure tanks, solved them for the wall thickness and added the needed thicknesses because we use CFRP as anisotropic material for the tanks.

$$\sigma_l = \frac{pR}{2\delta_l} \quad , \quad \sigma_t = \frac{pR}{\delta_t} \quad \rightarrow \quad \delta = \frac{3}{2}\frac{pR}{\sigma_{zul}} = \frac{3}{2} \cdot \frac{350\text{bar} \cdot 287\,\frac{\text{kJ}}{\text{kg K}}}{1000\text{MPa}} = 3.4\text{mm} \tag{22}$$

$$m_{Tank} = 200.9\text{kg} \quad , \quad m_{H2} = 21.4\text{kg} \quad , \quad m_{02} = 170.2\text{kg} \rightarrow \quad Q = 427.6\text{kWh} \tag{23}$$

The equation shows that the wall thickness is a linear function of the pressure. This results in a close to linear weight increase by increasing the pressure.

We have assumed a conservative tensile strength of 1000 MPa, including a safety factor of 2, which is far below the actual strength of CFRP with more than 2000 MPa. The certification could be done with the pressure tank standard. [31]

For the density of the hydrogen, we need to use the real gas equation because we are at relatively high pressures. When we compare the ideal gas and the real gas equation, we see that the gap between both is getting bigger with increasing pressure. The following diagram shows the difference between the real and the ideal gas density over the pressure.

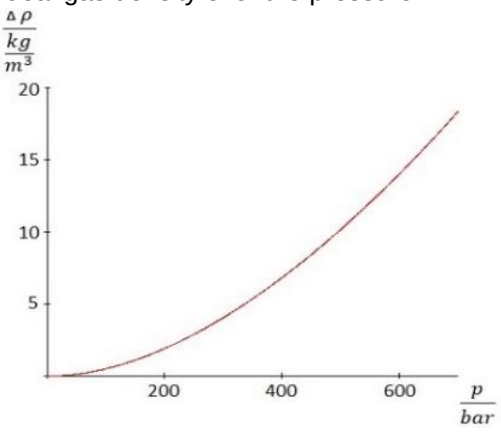

Fig. 4-20 Difference in density of hydrogen under pressure

The increasing gap between real and ideal gas densities leads to decreasing storage efficiency as the density doesn't increase linearly but the tank weight does. For our design process we chose a pressure of 350 bar as a good compromise between stored Hydrogen and tank weight. It's still worth mentioning that a change of this pressure at the detailed construction of the airplane is possible. For the size and amount of tanks we need to look at the airfoil of our wings.

The E216 airfoil Fig. 4-5 has space for 3 circular tanks with nearly identical diameter. A big challenge in the production of these tanks will be the decreasing diameter of the tanks because of the taper ratio of the wings. We know that this production will be challenging and more expensive but we are sure it's worth it.

Now with an assumption for the weight and energy capacity we are able to compare the use of hydrogen against batteries. For our airplane the most important value is endurance. Thus, we calculated the necessary energy for the climb to 20 km altitude and to get to the location of mission 1. The unknown value about the batteries is the energy density. To compare hydrogen and batteries we plotted the endurance over the energy density of the batteries and then we compared the endurance of our hydrogen configuration.

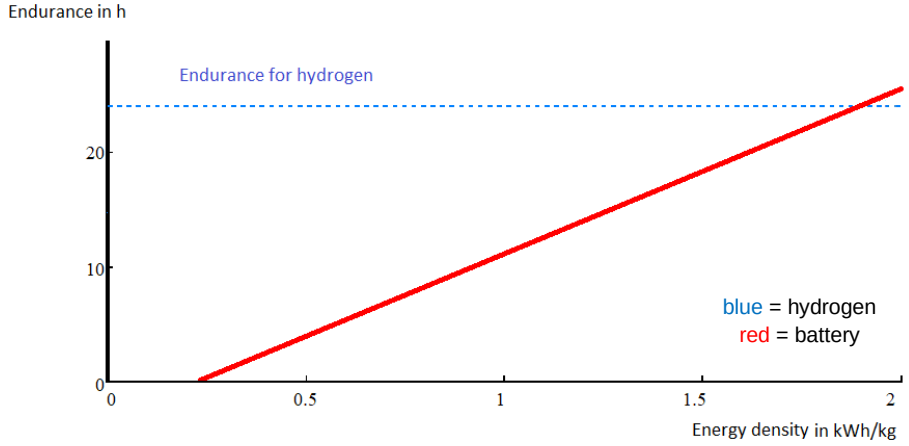

Fig. 4-21 Comparison energy density of battery and hydrogen

As one can see, the hydrogen (blue line) is superior to the battery (red line) until an energy density of 1.8 kWh/kg is reached. That is the reason why we chose hydrogen for our power system.

In summary, we will fly with a pressure of 350 bar, transporting in total 427.6 kWh of energy.

4.3.3 Thermal Management

Since our aircraft uses a hydrogen cell, which generates a lot of heat, and because our aircraft flies at altitudes where the air is very thin, it needs a lot of active cooling. The hydrogen fuel cell can generate 30 kW of power for our propellers with an efficiency of 60%. The critical point is shortly before reaching cruise altitude because we will need a power output of 30 kW, which means that a heat of 20 kW has to be dissipated. There will be an opening in the front of the plane through which 2 m^3/s of air for the cooling for the hydrogen cell will flow. In addition, it is possible to use the top of the fuselage, between the frame, to place radiators and ducts to increase the cooling as much as necessary. In further developments this topic needs to be developed further, so the systems do not overheat.

4.3.4 Propeller

Table 4-10 Propeller parameter

Name	Symbol	Value	Unit
required thrust	T_{req}	210	N
air density at cruise altitude	ρ	0.0879	kg/m³
diameter	D_{prop}	3	m
pitch	p_{prop}	2.19	m
efficiency	η	0.80	-
airspeed	v	55	m/s
cruise RPM	n_{RPM}	1692	U/min
number of propellers	n_{prop}	3	-

The maximum efficiency should be reached at cruise speed. From the diagram Fig. 4-22 we see that the efficiency of a propeller with 2 blades runs towards a value between 80 and 82%. The efficiency starts to decrease at a *P/D* (pitch to diameter) ratio of about 1.7 to 1.8. The efficiency is mainly dependent on the propeller tip speed. Drag increases drastically as propeller speeds reach numbers close to Mach 1. That is why we have given ourselves the diameter of **3 meters** as design point.

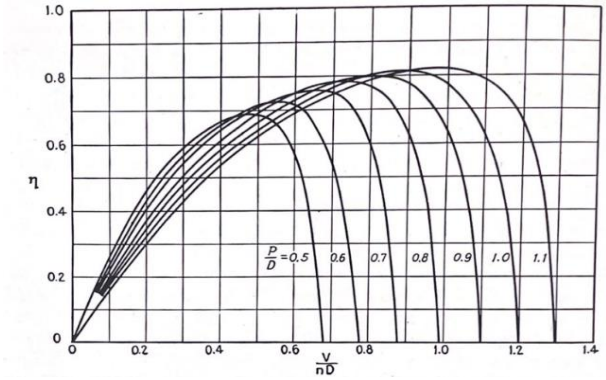

Fig. 4-22 Efficiency curves for simple propeller with 2 blades (P=Pitch) [32]

In the following ***P/D*$_{prop}$ equals *k*$_{prop}$**. After a few iterations we came to the conclusion that three propellers are ideal for us which means each propeller should provide 70 N of thrust. This results roughly in k_{prop}=0.8. In order to achieve maximum efficiency, we needed a relationship between k_{prop} and $\frac{v}{n_{RPS}D_{prop}}$. For us, this means $\frac{v}{n_{RPM}\,D_{prop}} = k_{prop} - 0.08$ for maximum efficiency.

$$n_{RPM}(k_{prop}) = \frac{v}{D_{prop}(k_{prop} - 0.08)}$$

With the dynamic thrust equation by Staples [32] we get:

$$F(k_{prop}) = \left(\frac{1}{3.29546 \cdot k_{prop}}\right)^{1.5} \rho \frac{\pi}{4} D_{prop}^2 \cdot \left[(n(k))^2 \cdot (k_{prop} \cdot D_{prop})^2 - n_{RPM}(k_{prop}) \cdot k_{prop} \cdot D_{prop} \cdot v\right] \quad (24)$$

As a result, we get the following diagrams for **maximum efficiency**:

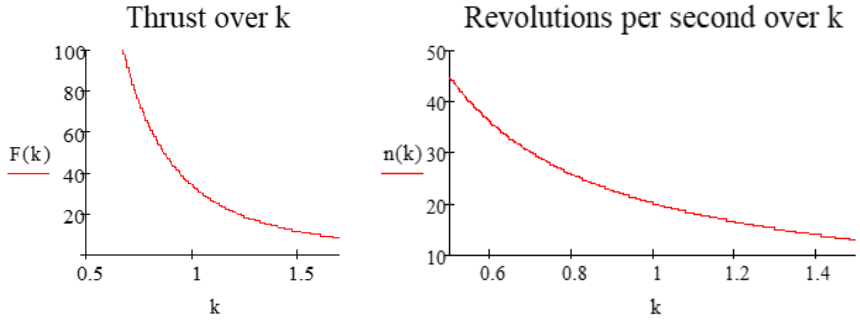

Fig. 4-23 Thrust and revolutions per second over *k*$_{prop}$

Given 70 N of thrust we get maximum efficiency 80 % at a k_{prop} of 0.73 and 28.2 U/s. This will be our cruise setup. Our propeller tip speed is 199 m/s which is far below the speed of sound. Special propeller blades designed especially for our demands would increase efficiency by a fair margin. Symmetrical thrust distribution is important. With 3 propellers, one propeller should be mounted in the centre and two on the wings. We have chosen the lower front wing to reduce the moment generated. For optimum efficiency, the propellers are mounted behind the wing so as not to disturb the airflow over the wing. [33]

4.4 Fuselage

The purpose of the fuselage is the storage of the payload modules, to connect the front and rear wing and the landing gear with each other, and to provide room for some of the other necessary modules that are needed for flight. The main considerations which drove the decision making were aimed at minimizing costs, weight, space and aerodynamic air resistance.
The overall length of the fuselage will be 6900 mm. This is necessary to make sure that the wings can be connected to the back of the fuselage.

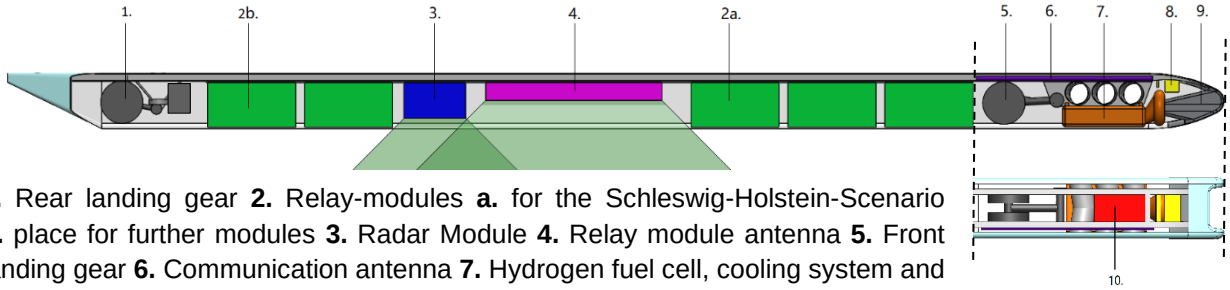

1. Rear landing gear **2.** Relay-modules **a.** for the Schleswig-Holstein-Scenario **b.** place for further modules **3.** Radar Module **4.** Relay module antenna **5.** Front landing gear **6.** Communication antenna **7.** Hydrogen fuel cell, cooling system and compressor **8.** Avionics **9.** Nose cone **10.** Emergency Battery (2 kWh)

Fig. 4-24 Layout of modules in the fuselage

4.4.1 Main Frame

The main frame has been designed to bear the loads of all the components that are attached to it and to transfer these loads to the wings or landing gear. In its heaviest configuration the frame is designed to carry at least 28 kg of weight. It also carries the avionics, the hydrogen cell and a compressor in the front of the plane.

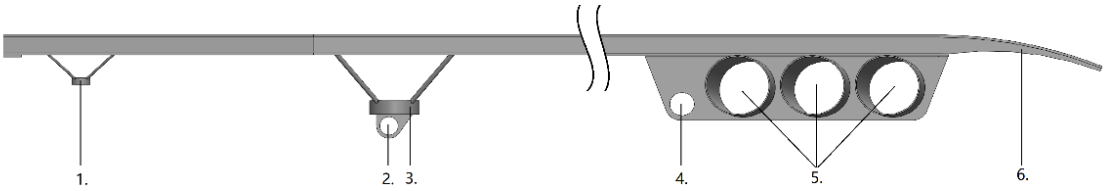

1. Front mounting point for rudder; **2.** Mounting point for the rear landing gear
3. Rear mounting for the rudder **4.** Mounting point for the front landing gear
5. Mounting point for wing 1 **6.** Mounting point for the nose cone

Fig. 4-25 Main frame – sideview

The wings are connected with three separate tubes, each with a span of around 3 m, which can be installed by a human with a few turns. These tubes are bended to match the dihedral angle and sweep angle of the wings. Afterwards, the wings halves are pushed onto the tubes, which are between the skin and around the pressure tanks, thus creating a tight connection. The wing is secured against self-disassembly with a new tensioner.
Wing 2 is mounted in a similar way. The mounting points are constructed with a clearance fit to ensure an uncomplicated installation of the tubes and to use different wing configurations.
Material choice – To fulfil this purpose the frame will be made from EN-AW 7020 [34]. AlTi alloys and EN-AW 7075 [35] have been considered. Both have advantages in specific strength over EN-AW 7020. [36] However, aluminium-titanium alloys are very difficult to machine and is therefore very expensive. It was decided that the potential savings in weight were not balanced out by the additional costs for using alloys. On the other hand, EN-AW 7075 cannot be welded in the way that we would like. Considering that some welding is needed to make the desired shape for the frame, the decision was made to abandon EN-AW 7075 as a possible material for the construction of the frame. The use of GLARE composites was considered, because of its superior specific strength. Due to its unique properties, the modelling of any frame made from this material is impossible with the knowledge and tools we have available. However, if further development is going occur the use of GLARE instead of aluminium for the main frame might be one way of reducing the weight of the frame.

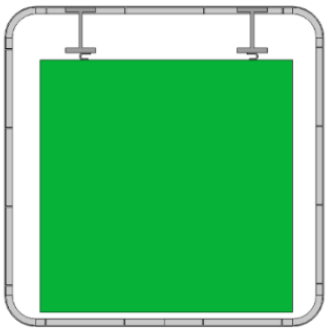

Fig. 4-26 Fuselage cross section

Cross section design – The hull has two parallel H-beams on the upper side, which are connected there and at the wing/rudder mounting points. (Fig. 4-26) The H-shape was chosen, because this shape has comparatively good resistance against bending moments, while also being cheap and requiring relatively little material. The double beam configuration with connections between the beams was chosen to create a corridor for airflow to the rear of the aircraft to reduce heat build-up. This design choice also increases the resistance against torsion moments from the rudder and provides a stable mounting place for the payload. Fuselage cross section

Mounting points – Both wings and the landing gear are integrated in the frame. The mounting points for the landing gear is mounted as close to the wing mounts as possible. This allows for a direct transportation of the load of the wing onto the landing gear. The mounting for the back wing and the rudder will be round and will be connected by a screw to the mounting to allow upward forces to be carried by it.

Front of main beams – This is bended in such a way that it reinforces the nose of the plane. The underside of the beam will be shaven off to make a T-beam. This decision has been made to save weight, because the loads on that part of the structure are smaller than those on the midsection of the plane.

Weight and loading – The whole structure has been calculated to carry a static load equal to the payload under a 2.1 g load (see chapter 4.6) and a safety factor of 1.5. This calculation has been performed on a sketch of the main frame with the Solidworks SimulationXpress Analysis Wizzard [37]. Based on that analysis the total weight of the frame must be 18.5 kg.

Landing gear weight – This has been calculated by analytical methods. Textbooks suggest that a normal landing gear assembly weights approximately up to 3.5% of the maximal take-off weight ($m_{TO,max}$). However due to the nature of the landing gear configuration it can be assumed that a penalty of 0.5 percentage points applies, but this might also be balanced out by the particularly short nature of the landing gear so that in the end the initial estimate of 3.5% of $m_{TO,max}$ will probably be a sufficiently accurate guess. The weight will likely be 19.5kg.

4.4.2 Hull

Material – This will be natural fibre reinforced composites (NFRCs) made from jute or other agricultural by-products. [38] These NFRCs have a relatively good strength to weight ratio, are cheap and easy to form, are comparatively resistant to damage and are very eco-friendly. NFRCs are also not electoral conductive, so they do not interfere with the (electro-magnetic) equipment on board. The drawbacks of these materials are that they are not very resistant to water and UV-light. This requires an application of a protective layer of paint or other protective measures. To ensure protection against lightning, a conductive aluminium mesh will be added to the outside of the hull at the appropriate places, though not under the radar and internet antenna. This has the added advantage that the plane complies with existing EASA regulations for similarly sized planes.

Hull shape – This has been designed with three main criteria in mind. The hull should be able to contain all the modules, be as aerodynamic as possible, while also being as cheap and as easy to maintain as possible. To achieve this the hull has been made rectangular (312 mm x 313 mm) with a fillet of 30 mm with a symmetric aerodynamic nose cone and a tapered tail section. At the bottom side of the nose there is an opening of 400 cm^2 in the nose to allow air to enter the hydrogen cell. In the rear and under the hydrogen cell there is an opening to allow the air from the hydrogen cell to exit. There are also additional holes at the places where the beams from the wing enter the hull. To allow for the installation of the payload, there will be a door installed on the side of the hull. Inside the hull there are a few ribs that are designed to stiffen the hull and allow it to keep its aerodynamic form. Just in front of the rudder, on the left side of the plane there is a large door through which the payload modules can enter the plane. Additionally, on top of the hull, there are three doors through which the maintenance crew can push the modules into their place.

The hull has been sketched in Solidworks [37]. There was a penalty calculated for the internal rib structure of $m_{hull} = 1.096 \cdot m_{solidworks}$.

This has been calculated by sketching a 1m-section of the hull with and without ribs and then dividing the weight for the hull with ribs through the weight of the hull without ribs. Consequentially estimate of its weight is 11.1 kg.

4.4.3 Integrated Structures

Payload – This will be fully integrated into the fuselage between the front and rear wing. The communications antenna will be integrated into the frame within the H-beam. All other payloads will be attached below the frame as to ensure that the H-beams will not interfere with the radar and internet antenna.
The modules can be attached to the payload by a rail system. The position of the payload may be locked with a small screw. This system improves the mobility of the payload, since the payload can be attached and moved around easily by hand, allowing easy repositioning of the payload modules. It is more precise compared to other systems we considered, although it is a bit heavier than those other methods. This also has the advantage of improving the modularity of the airplane as any payload-module that fits the specifications of our airplane could be attached to it.
Configurations – There are two possible configurations for both scenarios. In each scenario will be a radar module and one antenna-array module on the plane. The number of "Broadband internet relay modules" (BBIRM) varies between the two operations. [39] There will be one BBIRM for the Schleswig-Holstein scenario and four BBIRM for the Hamburg scenario. However, for scenarios outside of the design envelope, which can require different integration of the payloads, the plane can take up to five BBIRM. The total payload weight for the Holstein scenario is 13 kg, the total payload weight for the Hamburg scenario is 28 kg. The rail system allows the payload modules to be moved around inside the plane. With different payload configurations the payloads will be shifted around to keep the centre of gravity around the same point in the plane.

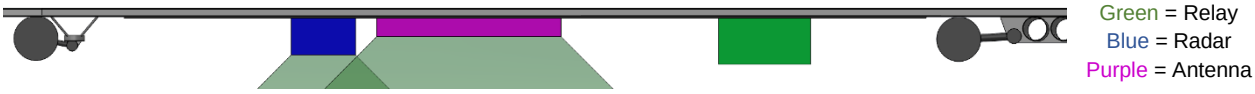

Fig. 4-27 Layout of the components for the Schleswig-Holstein Scenario

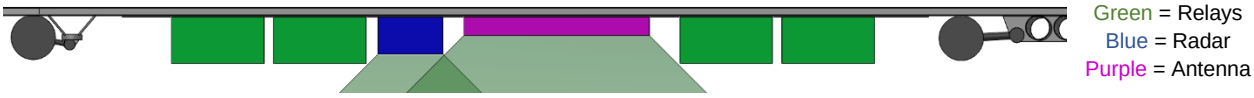

Fig. 4-28 Layout of the components for the Hamburg Scenario

Other mounted structures – In the nose of the airplane there will be an avionics bay installed. Additionally, there will be a removable lid made of aluminium which will protect the nose against possible strikes from the front of the plane. It is also the access-port for the avionics as well as the electronics and hydrogen cell in the front of the plane. This lid will also have a duct that feeds air to the hydrogen cell just behind it.
In the front of the plane, there will be a hydrogen cell installed, which is the main power source. This structure is just below the mounting of the front wing. Above the mounting and the hydrogen cell there is an emergency battery installed, which has a capacity of 2 kWh. Other structures might be installed in the plane if deemed necessary.

4.5 Avionics

The avionics on the plane are critical since the plane will operate remote controlled to save weight on the pilot and associated support systems. The avionics should both control the plane and furthermore conform to any possible regulations.
Autopilot – This will likely be a modified version of the WePilot3000 made by WeControl or a similar model of an autopilot. This autopilot has been chosen, because it has three gyroscopes, three accelerometers, one three axis magnetometer, absolute and differential pressure sensor and GPS/GLO sensors preinstalled. The deciding advantage of the system is the large temperature range in which it can safely operate (-40 °C – 80 °C). However, with a maximum power consumption of 18 W this system is relatively power hungry compared to competing autopilots. This system is, in our opinion, still the best in the market for our purposes [40] [41]

Transponder and "detect and avoid" system – There also will be a transponder [42] and detect and avoid system [43] installed to make sure that other aircraft can get advanced warnings of their proximity to this airplane. It will also make sure, that if another aircraft gets too close an automatic sequence is started, so that the risk of collision is minimized.
Other systems installed – Apart from the sensors pre-installed in the autopilot, there will be additional sensors installed to improve the situational awareness of the pilots. First of all, there will be two cameras installed in the plane; one in the nose of the plane to obtain a good view during landings. This camera might also be rigged in such a way, that it can look down for making photo images of the landscape below for reconnaissance. Additionally, there will be a second camera in the middle of the back wing, so the pilot can detect possible damage to the plane. Other sensors that will be installed are three pitot probes and three associated static pressure probes to accurately measure the airspeed and attitude of the airplane. If the radar-module is installed in the plane, it may also double as a ground radar to measure the direct distance between the plane and the ground, which mitigates the risk of a controlled flight into terrain.
If appropriate, the installation systems that allow a precision approach (like a lidar) may be considered to allow the airplane to safely operate in low visibility conditions like mist and rain. Lastly, LED beacon lights will be mounted on the appropriate places to ensure compliance with EASA regulations.

4.6 Certification

The chapter gives a short overview about a possible certification. We checked our aircraft for different EASA regulations, such the CS-22, CS-23 and CS-25, all of which are unfortunately not applicable for us in terms of flight envelopes. Nevertheless, a maximum load factor $n = 1.25 \cdot \left(\frac{v}{v_{stall}}\right)^2 = 2.1\ \mathrm{g}$ could be assumed according to CS-22.341 "Gust load factors".
In the future, we look forward to a new certification specification for high-flying autonomous unmanned aerial systems being established. Alternatively, we will need a specific type certification just for our aircraft, as Leichtwerk AG has done it with StratoStreamer for example. [44]
Due to our operating scenario at every weather condition, our wings are designed stiffer which is giving an advantage for load cases. In addition, our *AirShip* has a number of technologies (chapter 7.2) that have not been certified. Examples are the morphing wing and the pluggability of the whole aircraft.
Our plan is to build 5 test aircraft for to shorten the certification process, by testing different scenarios simultaneously.

5 Operating Concept

Fig. 5-1 *AirShip-E216* flying above Hamburg (h=20km)

Our aircraft will fly inconspicuously with their ice blue livery. The fleet concept consists of planes with shorter or lager fuselages. Some may have a completely different wing depending on their site of operation. For instance using solar cells in the Sahara and others will fly with an active de-icing system in polar regions. Thanks to its unique modularity, not only the payload but also the entire configuration can be changed to provide a new family fleet concept in aviation. The individual aircraft can fly a mission alone or in a family system.

Range / Endurance – These parameters are most important to fulfil the requirements.

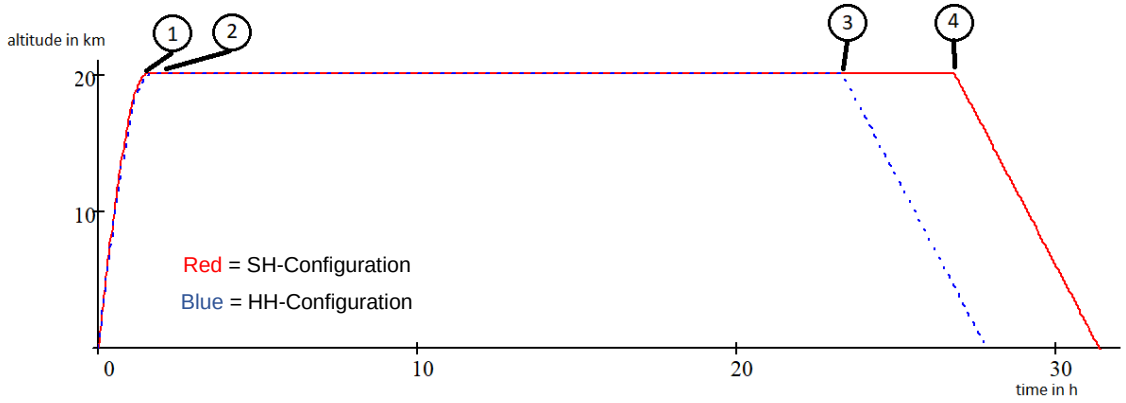

Fig. 5-2 Endurance diagram

The blue dotted line presents the heavy configuration for Hamburg and the red line the lighter configuration for Schleswig-Holstein. Point 1 represents the arrival at cruise altitude. The second point describes the arrival of our aircraft at the location of the mission. There are slightly differences in the numbers according to the configuration.

Table 5-1 Endurance diagram points

Hamburg

Point	*R* [km]	*t* [min]	*t* [h]
1	162	95	1.58
2	182	104	1.73
3	4561	1477	24.62

Schleswig-Holstein

Point	*R* [km]	*t* [min]	*t* [h]
1	148	92	1.54
2	182	102	1.70
4	5232	1980	28.00

In cruise flight one aircraft needs 14.35 kW of power. The last two points 3 and 4 are showing the endurance of our aircraft until the hydrogen tanks are empty. In this case, the return flight to the home base is by gliding. The achievable performances for loitering are 4902 km respectively 24.8 h for Hamburg and 4217 km respectively 21.3 h for Schleswig-Holstein.

In an emergency of our aircraft at cruise altitude, we would be able to glide a range of 488 km (264 nm) with a flight path angle of 2.34° considering ideal conditions and an airspeed of 55 m/s.

Airport – *AirLive* was designed to be as flexible as possible when it comes to its operating base. Therefore, all parts of the aircraft were designed to fit into standardized containers mentioned in chapter 3. Additionally, all facilities needed to operate the aircraft for pilots, ground crew, maintenance and even extra hydrogen infrastructure in case there is no local hydrogen system, could be installed in such containers. This makes it possible to easily transport the equipment via ship or road. With a cruise altitude of 20 km the line-of-sight distance will be estimated with the formula:

$$d \approx 4.12 \times \sqrt{h} \; = \; 582.66\,\text{km} = 314.61\,\text{nm} \tag{25}$$

Therefore, the ground station can be positioned at the operating airport. The chosen airport for the mission must be certified for landing at nights. If this is not the case, we can transport our own lights for the runway and the approach phase. During one operation the aircraft is operating out of one airport.

Take-off – We plan to start the aircraft remote controlled with a winch launch and the center prop already running. By doing this we gain height as fast as possible in order to start the other two props without spinning into the ground. The take-off speed is between the minimum speed, which is limited by stalling and the maximum speed, limited by loading on aircraft. If that specific speed cannot be hold, an immediate release of the tow is necessary. In this situation it is the pilot's task to prevent from further damage by continue flying remote controlled.

Cruise – During cruise flight the plane flies a preprogrammed route fully autonomous. All aircraft in one mission can and will communicate among each other to warn of dangers.

Landing – The landing will be done remote controlled by a pilot. He will be supported by an autonomous landing system with a 3D data transmitter and aircraft localizer like a LIDAR system. For the landing the bottom props will be locked in a horizontal position to make sure they will not hit the ground. This will happen in the last possible moment to insure a late, but safe go-around.

Ground Crew – The ground crew is responsible for refuelling, maintenance and fluent operation. The turnaround of an airplane lasts about 60 minutes. The machine has to be pulled of the runway, refuelled, the payload has to be checked and a walkaround has to be done. In case of a maintenance problem, we are planning to have 1.5 times the amount of planes needed to fly the mission.

5.1 Mission 1

Hamburg – To provide internet to all the 1.854 million inhabitants within the area of 755 km² we will need 3 aircraft with a maximum amount of 4 internet relays and a radar module per plane. With the aim of covering the whole region the aircraft will circle the city with a diameter of approximately 5 km (dotted line in the middle).
Each black circle presents the covered aera by one plane. The blue dotted circle shows the area, which is covered all the time.
Schleswig-Holstein – For this scenario up to 50 planes will be needed to cover the entire area of 15.804 km² constantly. They will be equipped with 1 internet relay per plane and one radar module. These aircraft will fly a pre-programmed route. The shown route in Fig 5-3 has a total length of 1000 km. All aircraft would fly 20 km apart. By doing this, the planes will continuously cover a 34.64 km wide quadrangular shape along the route. Please note that this route is an example and has to be optimized or a stationary flight path has to be taken into account.

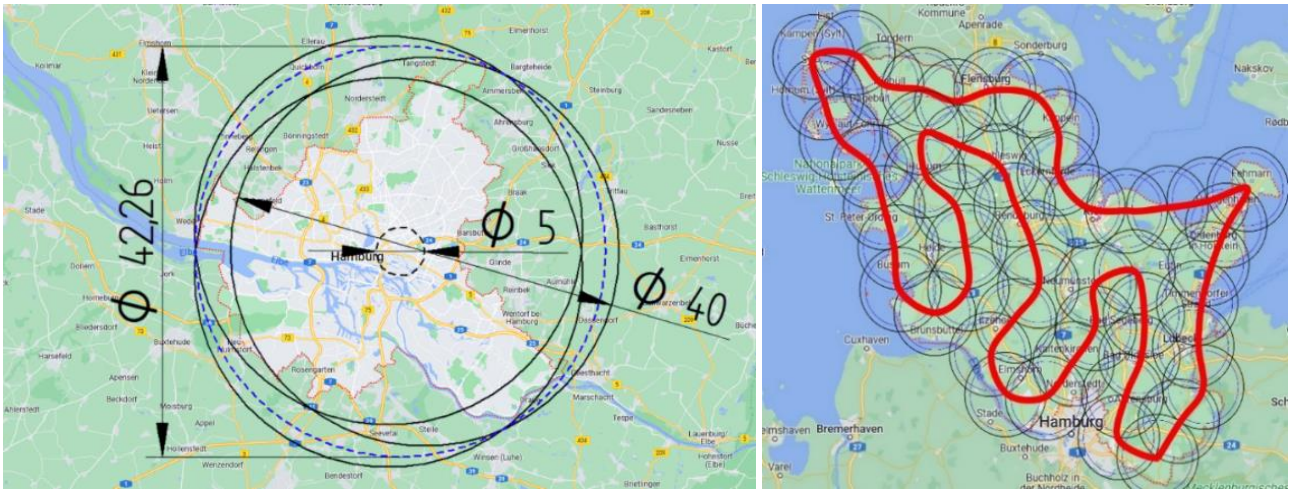

Fig. 5-3 Mission 1 Hamburg (left) and Schleswig-Holstein (right)

5.2 Mission 2

For this mission we will use one plane from mission 1. The rest of the fleet is still capable of covering Hamburg and Schleswig-Holstein with mobile infrastructure. To fly the distance of 170 nm it will take us about 116 min including a headwind of 10 m/s and an airspeed of 55 m/s. The flying aircraft with less than 75% of energy will still have a remaining range 4432 km (2393 nm) without any payload running. That corresponds to an endurance of 22.4 h. If the design payload systems are using 1 kW of energy, the range reduces to 4156 km or 21.0 h in endurance. In a configuration for Hamburg the payload systems will use 3 kW, which reduces the performance to 3676 km and 18.6 h. To start a spare aircraft, it will take the ground crew about 15 min.

5.3 Other Applications

Besides the emergency communication and observation missions *AirLive* is capable of flying various other operations. Observation flight could also be done for agricultural use or research. Furthermore, they could support search and rescue operations in semi remote areas like forests or lakes. By equipping the aircraft with other modules, it could additionally be used for weather pattern research or even military observation and detection. Another special mission would be in the arctic to measure in different altitude simultaneously. The system provides bandwidth for major sporting events and festivals such as the 24h race at the Nürburgring or the “Medimeisterschaften”. It is thinkable to change the maximum take-off weight in relation of the wing loading.

5.4 Emergency Situations

Safety and reliability are key features to ensure a user friendly and safe system. In case of an emergency on our aircraft, it is most important that no life will be threatened. In the event of an engine failure due to the high glide factor of the aircraft, there will still be a lot of range left. If the aircraft is not safe to land, it is always possible to change its course to the direction of uninhabited places like seas, oceans or fields. In addition, it will be possible to connecting several aircraft to fly like a flock of birds. The leading aircraft will be controlled by a pilot. In case of failure in communication, the plane starts a preprogramed autonomous routine by reducing the altitude and flying closer to the next ground station. If the problems remain after reboot mid-air the aircraft will redirect to the starting point for an autonomous emergency landing with our own 3D-landing system.

6 Costs Analysis

For the success of our concept, it is necessary that our aircraft can be used in the system in an economically profitable way by the operator. We have divided our costs into operational and aircraft costs. This is a rough first estimate. The calculations were made on the basis of the present mission. We have largely followed the DAPCA-IV model and estimated many other factors through active discussion. [18] Our calculations are based on the assumption that we sell a **total of 1000 aircraft**. We have a "**safety factor" of 1.5** (for inflation etc.) and a profit margin of 20% on each aircraft sold.

Major operational costs are crew, aircraft insurance, fuel, fees and infrastructure. The latter includes the rental of the airfield and costs for secure servers and communication lines. The cost per crew member is on average 100 €/h. The insurance sum is 1/3 of the acquisition costs spread over a period of 20 years. The price of hydrogen is calculated at 10 €/kg. Probably the market price will be lower in 2040, but costs will increase due to poor availability at many airfields.

Table 6-1 Estimated costs for production and operation

Aircraft costs	**Price**	**Unit**
Factory	250,000,000	€
Labour costs	230,000	€/AC
Material costs	71,800	€/AC
Production costs	440,000	€/AC
Certification costs	40,000,000	€
Software	20,000,000	€
Marketing	40,000,000	€
Total (with safety-factor of 1.5)	**1,637,700**	**€/AC**
Purchase Price (per plane)	**2,000,000**	**€/AC**

Operating Costs	**Price [€/d]**
Crew	84,800
Insurance	2,700
Fuel	15,000
Fees	5,000
Infrastructure	7,000
Maintenance	1,000
Total	**173,250**

Our labour costs are made up of development work and assembly work. The average hourly wage is also 100 €. Since our production is to be highly automated, we need a new, state-of-the-art factory for which we have determined the costs using the costs of new car factories. The certification process will require several aircraft that are very expensive to produce. Labour costs for the process are not included in this cost. The current production costs are significantly higher. Especially the production of complex composite parts is very expensive with up to 20,000 €/m². Here we expect prices to quarter on average over our production period.

7 Conclusion

After long and thoughtful elaboration, we developed a system of aircraft for crisis situations meeting all requirements. We are confident that this concept might be operational under all conditions until 2040.

However, Mission 2 has presented us many challenges, leading to rising costs in all areas. The high-speed requirement demands a high degree of stability and prevents the use of zeppelins or ultra-light solar-powered aircraft. Our system can be purchased by operators, such as governments, who wish to operate independently from private satellite operators. Our advantage is the fast availability of our system, in comparison to ground systems. The best part of our cost-efficient concept is the modularity of the whole aircraft for future tasks and improvements with state-of-the-art efficiency. This way we can operate many kinds of missions with varying payload, which makes our fleet even more environmentally friendly.

7.1 Requirement fulfilment

Table 7-1 Overview of the requirements

#	Requirement	*AirShip-E216*	achievement
1	serve Hamburg (HH) in mission 1	3 planes used	achieved
2	serve Schleswig-Holstein (SH) in mission 1	50 planes used	achieved
3	short time until internet is recovered	100 min (without headwind)	achieved
4	family fleet concept	Modular Structure of the aircraft	achieved
5	each aircraft must be able to fly from basis on its own		achieved
6	time of loitering at 20 km to provide internet	at least 21.3 hours/aircraft	achieved
7	return to base after missions	even with gliding possible to fly 264 km	achieved
8	serve mission 2 during mission 1 (HH)	1 of 3 planes will take the mission	achieved
9	serve mission 2 during mission 1(SH)	1 of the planes will take the mission	achieved
10	fly 170 nm in under 2 h to mission 2 with less than 75 % energy left	-with 75 % we have a range of 4494 km -we will be at mission 2 after 116 min with headwind	achieved
11	low emissions, environmentally friendly	green hydrogen power system and natural fibres	achieved
12	system for collision avoidance in autonomous flight	flight computer, autopilot, lidar, transponder	achieved
13	fly in all weather conditions	strong wing structure, use of de-icing strategy	achieved
14	fly at any time of the day	time independent power system	achieved
15	fly at 55° latitude north	no solar cells installed	achieved
16	EIS 2040		planned

7.2 Future Technologies

Table 7-2 List of future technologies used in our concept

#	Name	TRL	explanation	Why available until EIS 2040?
1	Modularity of the whole aircraft structure	9	gliders are pluggable	-only special connecting solutions for the wings are necessary
2	Morphing wing	7	tests run by NASA [19]	-currently under testing and a lot of research on this topic
3	Conic Hydrogen pressure tanks	3	no information about research to maximize volume in wing for pressurized tanks	-conical tubes for structural purposes are available, so it would be possible to develop a process to make pressure tanks
4	Mobile 3D lidar system for autonomous landings	6	autonomous landings in tests successful [45]	-software and hardware will improve a lot until 2040
5	Sharkskin as an option for customers	9	on the market since 2022 [16]	-will become cheaper by 2040 due to decreasing production costs
6	New environmentally friendly de-icing fluid	8	on the market are recycling systems for de-icing fluids [46]	-new environmentally friendly chemical fluids are being researched in all industries
7	aircraft flying like a flock of birds	4	tests run by combat aircraft, like drones (FCAS) [47]	-high military interests to reduce the number of pilots on combat mission

8 References

[1] “Anzahl der weltweiten Naturkatastrophen,” Statista, [Online]. Available: https://de.statista.com/statistik/daten/studie/249326/umfrage/anzahl-der-weltweiten-naturkatastrophen/. [Accessed 05 07 2023].

[2] “Flightglobal,” [Online]. Available: https://www.flightglobal.com/defence/airbus-readies-high-flying-zephyr-for-2024-service-launch/151546.article. [Accessed 05 06 2023].

[3] A. Bierig, “EDU,” DLR, [Online]. Available: https://und.edu/research/soars/_files/presentations/dlr.pdf. [Accessed 05 06 2023].

[4] “HAPS,” Leichtwerk AG, [Online]. Available: https://www.leichtwerk.de/fileadmin/start/HAPS_WhitePaper_A11_e.pdf. [Accessed 05 06 2023].

[5] “AirForce,” [Online]. Available: https://www.af.mil/About-Us/Fact-Sheets/Display/Article/104516/rq-4-global-hawk/. [Accessed 05 06 2023].

[6] DFS Deutsche Flugsicherung GmbH, 13 04 2023. [Online]. Available: https://aip.dfs.de/datasets/. [Accessed 05 05 2023].

[7] “Securecontainer,” [Online]. Available: https://www.securecontainer.ca/shipping-container-dimensions/. [Accessed 29 06 2023].

[8] “Wearedg,” [Online]. Available: https://wearedg.com/news/article/teu-and-feu-containers. [Accessed 29 06 2023].

[9] P. Horst, C.-C. Rossow and K. Wolf, Handbuch der Luftfahrtzeugtechnik, Munich: Hanser, 2020.

[10] D. Scholz, “Induced Drag Estimation of Box Wings,” Hamburg University of Applied Sciences, Darmstadt, 2019.

[11] D. Schiktanz and D. Scholz, “BOX WING FUNDAMENTALS – AN AIRCRAFT DESIGN PERSPECTIVE,” Hamburg University of Applied Sciences, Hamburg, 2011.

[12] “E216,” [Online]. Available: http://airfoiltools.com/airfoil/details?airfoil=e216-il. [Accessed 29 06 2023].

[13] “ClarkY,” [Online]. Available: http://airfoiltools.com/airfoil/details?airfoil=clarky-il. [Accessed 29 06 2023].

[14] “NACA0012,” [Online]. Available: http://airfoiltools.com/airfoil/details?airfoil=n0012-il. [Accessed 29 06 2023].

[15] OpenVSP, 10 01 2012. [Online]. Available: https://openvsp.org/. [Accessed 04 04 2023].

[16] “Lufthansa Technik,” [Online]. Available: https://www.lufthansa-technik.com/en/aeroshark. [Accessed 28 06 2023].

[17] P. O. Jemitola and P. P. Okonkwo, “An Analysis of Aerodynamic Design Issues of Box Wing,” Global Journals, 2022.

[18] P. D. Raymer, Aircraft Design: A Conceptual Approach, Washington, DC: AIAA, 1989.

[19] “nasa-successfully-tests-shape-changing-wing-for-next-generation-aviation,” 28 04 2015. [Online]. Available: https://www.nasa.gov/press-release/nasa-successfully-tests-shape-changing-wing-for-next-generation-aviation. [Accessed 05 05 2023].

[20] “Aircraft Stability,” [Online]. Available: https://www.cfinotebook.net/notebook/aerodynamics-and-performance/aircraft-stability. [Accessed 30 06 2023].

[21] APUS-Aero, [Online]. Available: https://group.apus-aero.com/. [Accessed 06 07 2023].

[22] M. V. Cook, Flight Dynamics Principles, Burlington, USA: Elsevier Ltd., 2007.

[23] B. Keidel, “Auslegung und Simulation von hochfliegenden, dauerhaft stationierbaren Solardrohnen,” Technische Universität München, München, 2000.

[24] “Adventure,” [Online]. Available: https://aroundtheworld.solarimpulse.com/adventure. [Accessed 20 05 2023].

[25] “Wirkungsgrad von CIGS Dünnschicht Solarzellen,” [Online]. Available: https://www.strom-forschung.de/projekte/photovoltaik/wirkungsgrad-von-cigs-duennschicht-solarzellen-durch-alkalibehandlung-steigern/. [Accessed 20 05 2023].

[26] “AIRBATT Solar-Power SFL 7.5 solar module set,” [Online]. Available: https://airbatt.de/AIRBATT-Solar-Power-SFL-75-solar-module-set-set-of-2. [Accessed 20 05 2023].

[27] “CIGS,” [Online]. Available: https://www.energie-experten.org/erneuerbare-energien/photovoltaik/solarmodule/cigs,%20. [Accessed 20 05 2023].

[28] “Solarflugzeug,” [Online]. Available: https://de.wikipedia.org/wiki/Solarflugzeug. [Accessed 20 05 2023].

[29] “Toyota Mirai,” [Online]. Available: https://en.wikipedia.org/wiki/Toyota_Mirai#:~:text=Each%20stack%20comprises%20370%20(single,cells%20on%20sale%20in%20Japan.. [Accessed 05 07 2023].

[30] “Apus i-2,” Apus Group, [Online]. Available: https://group.apus-aero.com/wp-content/uploads/2021/09/APUS_i-2_20210901.pdf. [Accessed 05 07 2023].

[31] “Merkblätter,” AD-2000, [Online]. Available: https://www.ad-2000-online.de/de/inhalt/enthaltene-ad-2000-merkblaetter. [Accessed 09 07 2023].

[32] “Propeller static dynmic thrust equation background,” 01 06 2015. [Online]. Available: https://www.electricrcaircraftguy.com/2014/04/propeller-static-dynamic-thrust-equation-background.html. [Accessed 07 06 2023].

[33] G. Hildebrandt, “Der Propeller,” [Online]. Available: https://www.fmsv-grossbreitenbach.de/doc/Motor.pdf. [Accessed 06 07 2023].

[34] Nedal Aluminium, “alloy data sheet,” 30 06 2023. [Online]. Available: https://www.nedal.com/wp-content/uploads/2017/11/Nedal-alloy-Datasheet-EN-AW-7020.pdf.

[35] Gleich Aluminium, “Al Rolled Plates EN AW - EN AW 7075 Technical Data sheet,” 30 06 2023. [Online]. Available: https://gleich.de/wp-content/uploads/2021/03/en_en_aw_7075-02-19.pdf.

[36] Nedal Aluminium, “alloy data sheet,” [Online]. Available: https://www.nedal.com/wp-content/uploads/2017/11/Nedal-alloy-Datasheet-EN-AW-7020.pdf. [Accessed 30 06 2023].

[37] Solidworks, Solidworks SimulationXpress Analysis Wizzard, 2022.

[38] A. A. R. Z. U. A. W. A. H. A. Muhammad Yasir Khalid, “Natural fiber reinforced composites: Sustainable materials for,” *Results in Engineering,* p. 12, 2021.

[39] “ITU,” [Online]. Available: https://life.itu.int/radioclub/rr/art1.pdf. [Accessed 05 06 2023].

[40] WeControl, 06 06 2023. [Online]. Available: https://www.wecontrol.ch/user/pages/products/wePilot3000/flyer_wePilot3000.pdf.

[41] WeControl, 06 06 2023. [Online]. Available: https://www.wecontrol.ch/user/pages/products/wePilot3000/flyer_wePilot3000.pdf.

[42] Avioni, “Ping200XR,” 30 06 2023. [Online]. Available: https://uavionix.com/products/ping200xr/.

[43] Avioni, “PingRXpro,” 30 06 2023. [Online]. Available: https://uavionix.com/products/pingrx-pro/#faqs.

[44] “High Altitude Platform,” Leichtwerk AG, [Online]. Available: https://www.leichtwerk.de/. [Accessed 03 07 2023].

[45] “2020-06-airbus-concludes-attol-with-fully-autonomous-flight-tests,” Airbus, 05 06 2020. [Online]. Available: https://www.airbus.com/en/newsroom/press-releases/2020-06-airbus-concludes-attol-with-fully-autonomous-flight-tests. [Accessed 08 07 2023].

[46] “Efficient recycling of de-icing fluids,” Munich Airport, 16 12 2019. [Online]. Available: https://www.munich-airport.com/international/eco-friendly-de-icing-at-munich-airport#:~:text=Munich%20Airport%20remains%20the%20only,when%20conditions%20ar%20especially%20harsh.. [Accessed 08 07 2023].

[47] “future-combat-air-system-fcas,” Airbus, [Online]. Available: https://www.airbus.com/en/products-services/defence/multi-domain-superiority/future-combat-air-system-fcas. [Accessed 08 07 2023].

[48] L. Boccia, P. Pace, G. Amendola and G. D. Massa, “Low multipath antennas for GNSS-based attitude determination systems applied to high-altitude platforms,” Springer-Verlag, 2008.

[49] A. Badis, “Subsonic Aircraft Wing Conceptual Design,” International Journal of Sciences: Basic and Applied Research, Algeria, 2017.